



**UNIVERSIDAD DE INVESTIGACIÓN DE
TECNOLOGÍA EXPERIMENTAL YACHAY**

Escuela de Ciencias Químicas e Ingeniería

**TÍTULO: Modified Chitosan Films with CPH-based
additives for Food Packing Applications**

Trabajo de integración curricular presentado como requisito
para la obtención de título de Químico

Autor:

Katherine Andrea García Pinos

Tutores:

Manuel Caetano, Ph.D.

Lola De Lima, MSc.

Urququí, Julio 2022

SECRETARÍA GENERAL
(Vicerrectorado Académico/Cancillería)
ESCUELA DE CIENCIAS QUÍMICAS E INGENIERÍA
CARRERA DE QUÍMICA
ACTA DE DEFENSA No. UITEY-CHE-2022-00034-AD

A los 27 días del mes de junio de 2022, a las 14:00 horas, de manera virtual mediante videoconferencia, y ante el Tribunal Calificador, integrado por los docentes:

Presidente Tribunal de Defensa	Dra. LOPEZ GONZALEZ, FLORALBA AGGENY , Ph.D.
Miembro No Tutor	Dra. MICHELL URIBE, ROSE MARY RITA , Ph.D.
Tutor	Dr. CAETANO SOUSA MANUEL , Ph.D.

El(la) señor(ita) estudiante **GARCIA PINOS, KATHERINE ANDREA**, con cédula de identidad No. **0302450002**, de la **ESCUELA DE CIENCIAS QUÍMICAS E INGENIERÍA**, de la Carrera de **QUÍMICA**, aprobada por el Consejo de Educación Superior (CES), mediante Resolución **RPC-SO-39-No.456-2014**, realiza a través de videoconferencia, la sustentación de su trabajo de titulación denominado: **MODIFIED CHITOSAN FILMS WITH CPH-BASED ADDITIVES FOR FOOD PACKING APPLICATIONS**, previa a la obtención del título de **QUÍMICO/A**.

El citado trabajo de titulación, fue debidamente aprobado por el(los) docente(s):

Tutor	Dr. CAETANO SOUSA MANUEL , Ph.D.
Co - Tutor	Mgs. DE LIMA ELJURI, LOLA MARIA

Y recibió las observaciones de los otros miembros del Tribunal Calificador, las mismas que han sido incorporadas por el(la) estudiante.

Previamente cumplidos los requisitos legales y reglamentarios, el trabajo de titulación fue sustentado por el(la) estudiante y examinado por los miembros del Tribunal Calificador. Escuchada la sustentación del trabajo de titulación a través de videoconferencia, que integró la exposición de el(la) estudiante sobre el contenido de la misma y las preguntas formuladas por los miembros del Tribunal, se califica la sustentación del trabajo de titulación con las siguientes calificaciones:

Tipo	Docente	Calificación
Tutor	Dr. CAETANO SOUSA MANUEL , Ph.D.	10,0
Presidente Tribunal De Defensa	Dra. LOPEZ GONZALEZ, FLORALBA AGGENY , Ph.D.	10,0
Miembro Tribunal De Defensa	Dra. MICHELL URIBE, ROSE MARY RITA , Ph.D.	9,8

Lo que da un promedio de: **9.9 (Nueve punto Nueve)**, sobre 10 (diez), equivalente a: **APROBADO**

Para constancia de lo actuado, firman los miembros del Tribunal Calificador, el/la estudiante y el/la secretario ad-hoc.

KATHERINE ANDREA
 GARCIA PINOS
Firmado digitalmente por
 KATHERINE ANDREA GARCIA PINOS
 Fecha: 2022.07.20 17:35:48 -05'00'

GARCIA PINOS, KATHERINE ANDREA
Estudiante

FLORALBA AGGENY
 AGGENY LOPEZ GONZALEZ
 LOPEZ GONZALEZ
Digitally signed by FLORALBA
 AGGENY LOPEZ GONZALEZ
 Date: 2022.07.18 13:40:08
 -05'00'

Dr. LOPEZ GONZALEZ, FLORALBA AGGENY , Ph.D.

Presidente Tribunal de Defensa



Firmado electrónicamente por:
**MANUEL
 CAETANO**

Dr. CAETANO SOUSA MANUEL , Ph.D.

Tutor



Firmado electrónicamente por:
**ROSE MARY
 RITA MICHELL
 URIBE**

Dr. MICHELL URIBE, ROSE MARY RITA , Ph.D.

Miembro No Tutor

MARIELA
SOLEDAD
D YEPEZ
MERLO

Firmado digitalmente por MARIELA SOLEDAD YEPEZ MERLO
Fecha: 2022.06.27 16:14:49 -05'00'



YEPEZ MERLO, MARIELA SOLEDAD
Secretario Ad-hoc

To my beloved Mother

Autoría

Yo, **Katherine Andrea García Pinos**, con cédula de identidad 030245000-2, declaro que las ideas, juicios, valoraciones, interpretaciones, consultas bibliográficas, definiciones y conceptualizaciones expuestas en el presente trabajo; así cómo, los procedimientos y herramientas utilizadas en la investigación, son de absoluta responsabilidad de el/la autor (a) del trabajo de integración curricular. Así mismo, me acojo a los reglamentos internos de la Universidad de Investigación de Tecnología Experimental Yachay.

Urququí, Julio 2022

Katherine Andrea García Pinos

CI: 030245000-2

Autorización de Publicación

Yo, **Katherine Andrea García Pinos**, con cédula de identidad 030245000-2, cedo a la Universidad de Investigación de Tecnología Experimental Yachay, los derechos de publicación de la presente obra, sin que deba haber un reconocimiento económico por este concepto. Declaro además que el texto del presente trabajo de titulación no podrá ser cedido a ninguna empresa editorial para su publicación u otros fines, sin contar previamente con la autorización escrita de la Universidad.

Asimismo, autorizo a la Universidad que realice la digitalización y publicación de este trabajo de integración curricular en el repositorio virtual, de conformidad a lo dispuesto en el Art. 144 de la Ley Orgánica de Educación Superior.

Urcuquí, Julio 2022

Katherine Andrea García Pinos

CI: 030245000-2

Acknowledgements

First and foremost, I would like to thank God, who has endowed me with countless blessings, knowledge, and opportunities to finally accomplish my bachelor's degree. I want to extend my deepest gratitude to my advisors Lola De Lima, MSc. and Manuel Caetano, PhD., for their unwavering support, patient guidance, insightful suggestions, and precious time guiding me during this project. I would also like to express my most profound appreciation to my dear Professors and laboratory staff at the School of Chemical Sciences and Engineering for their invaluable guidance over these years. Many thanks to the School of Biological Sciences and Engineering and School of Earth Sciences, Energy and Environment, especially to Elizabeth Mariño, which cordially opened their facilities and allowed me to use the necessary equipment to conduct this research. My most profound gratitude and tremendous appreciation are presented to my beloved mother, Bertha, for her never-ending support, care, and love to encourage me to pursue my goals. This achievement will always be yours more than mine. My greatest thanks should also go to all my dearest relatives who continuously motivate me to accomplish this goal, especially my grandmother, Maria. To all my aunts and uncles for their words of encouragement that make me want to be your proud. Furthermore, thank my cousins, who always make me laugh and give me a purpose to continue, especially my darling Fabiana. Last but not least, I would like to thank all of my beloved friends for being part of this beautiful journey at Yachay Tech. Especially Adrian and Andy, you guys were my first friends and will always be the best ones I could ever ask. It does not matter where our future will take us; we already know that distance cannot take us apart. Salome, you always will have a piece of my heart; thank you for becoming my sister and sharing all the good and the bad that college brings us. Also, Naomi and Jean Carlos for the precious time in the final stretch of our college life. And finally, to my favorite guys who fulfilled the long writing nights and my breakdowns with their music.

Katherine Garcia Pinos

Resumen

Las películas de quitosano diseñadas con la adición de fillers han sido ampliamente estudiadas por su potencial aplicación en numerosos campos. En este proyecto, se prepararon películas de quitosano utilizando aditivos extraídos de la cáscara de la mazorca de cacao (CPH). Como matriz se utilizó quitosano de alto peso molecular y como aditivos funcionales nano cristales de celulosa (CNC), nano celulosa di aldehído (DANC) y extractos fenólicos (PCPH). Estos aditivos se utilizaron para mejorar las propiedades mecánicas y de barrera del quitosano. El enfoque de esta tesis fue la extracción de aditivos CPH para el procesamiento y caracterización de películas para aplicaciones de envasado de alimentos. La celulosa se extrajo mediante tratamiento alcalino combinado con blanqueo e hidrólisis enzimática. Los análisis FTIR y los estudios de difracción de rayos X revelaron que el tratamiento alcalino resultó en la obtención de celulosa de alta cristalinidad, mientras que el enzimático da como resultado la holocelulosa. Los tres aditivos se mezclaron por separado con quitosano como matriz y glicerol como plastificante a diferentes radios para obtener películas homogéneas a excepción de la formulación con DANC. El estudio de microscopía no mostró agregaciones de CNC, pero lo hizo para DANC en una escala micro. El entrecruzamiento se realizó eficientemente en películas DANC formando una base Schiff. Las pruebas mecánicas revelaron una disminución de la resistencia a la tracción del quitosano al agregar un 0,5% de glicerol y aditivos, mostrando un mejor rendimiento al agregar un 3% de CNC. Todas las formulaciones pueden ser bloqueadores UV. Además, las propiedades de barrera mejoraron ligeramente al agregar CNC y DANC, mientras que las películas formuladas con PCPH revelaron la inhibición del crecimiento de moho. Las películas a base de quitosano tienen el potencial de usarse en la industria alimentaria como materiales de bioempaque, con la posibilidad de mejorarse para actuar como empaque inteligente.

Palabras clave: *cáscara de la mazorca de cacao, quitosano, nanocompositos*

Abstract

Chitosan films designed with the addition of fillers have been widely studied for their potential application in numerous fields. In this project, chitosan nanocomposite films were prepared using additives extracted from cocoa pod husk (CPH). High molecular weight chitosan was used as the matrix, and cellulose nanocrystals (CNC), dialdehyde nanocellulose (DANC), and phenolic extracts (PCPH), as the functional additives. These additives were used to improve the chitosan's mechanical and barrier properties. The focus of this thesis was the extraction of CPH-additives for the processing and characterization of films for food packing applications. Cellulose was extracted via alkaline treatment combined with bleaching and enzymatic hydrolysis. FTIR analysis and X-ray diffraction studies revealed alkaline treatment derivatives in high crystalline cellulose, while the enzymatic one results in holocellulose. The three additives were blended separately with chitosan as a matrix and glycerol as a plasticizer at different ratios to obtain homogeneous films except for the DANC formulation. The microscopy study showed no CNC aggregations but did it for DANC on a micro-scale. Crosslinking was efficiently performed on DANC films by forming a Schiff base. Mechanical testing revealed decreased chitosan's tensile strength by adding 0.5% glycerol and additives, showing better performance at the addition of 3% CNC. All formulations can be UV-blockers. Moreover, barrier properties slightly improved by adding CNC and DANC, while PCPH formulated films reveal inhibition of moho growth. Chitosan-based films have the potential to be used in the food industry as bio packaging materials, with the chance to be improved to act as active packing.

Keywords: *cocoa pod husk, chitosan, nanocomposites*

Table of Contents

<i>Contents</i>	<i>Page</i>
Acknowledgments	iv
Resumen	vi
Abstract	viii
List of Figures	xiii
List of Tables	xv
List of Symbols	xvii
1 Introduction	1
1.1 Research context	3
1.2 Objectives	4
1.2.1 Main Objective	4
1.2.2 Specific Objectives	4
2 Theoretical Frame Work	5
2.1 Food packing	5
2.1.1 Biopacking	5
2.1.2 Biodegradation	6
2.1.3 Composting	7
2.1.4 Packing properties	7
2.1.5 Forms of biodegradable packaging	8
2.2 Added value products from CPH	9
2.2.1 Production and composition of CPH	9

2.2.2	CPH for the formulation of biocomposites	11
2.3	Chitosan	11
2.3.1	Extraction process of chitin and chitosan	11
2.3.2	Properties of chitosan	13
2.4	Cellulose	13
2.4.1	Extraction from agricultural waste	14
2.4.2	Nanocellulose	14
3	Experimental	17
3.1	Reagents and Equipment	17
3.1.1	Biological material	17
3.1.2	Equipment	17
3.1.3	Materials and chemicals	17
3.2	Sample preparation	18
3.3	Cellulose extraction	18
3.3.1	Pretreatment	18
3.3.2	Bleaching	19
3.4	Cellulose size decreasing	19
3.5	Cellulose oxidation	19
3.6	Phenolic extraction	19
3.7	Films preparation	20
3.7.1	Chitosan and CNC nanocomposites	20
3.7.2	Chitosan and DANC nonocomposites	20
3.7.3	Chitosan and PCPH	21
3.8	Characterization	21
3.8.1	X-ray diffraction (XRD)	21
3.8.2	Fourier-transform infrared spectroscopy (FTIR)	21
3.8.3	Scanning electron microscopy (SEM)	21
3.8.4	Solubility	21
3.8.5	Moisture absorption	22
3.8.6	Optical Transmittance Measurement	22
3.8.7	Mechanical properties	22
3.8.8	Packaging of blackberries	22
4	Results	25
4.1	Pectin enzymatic extraction	25
4.2	Cellulose extraction	26
4.3	Cellulose size decreasing: CNC	31
4.4	Cellulose Oxidation	35

4.5	Chitosan based biofilms	37
4.5.1	Film appearance and thickness	37
4.5.2	FT-IR of films	39
4.5.3	Morphology of films	41
4.5.4	Mechanical properties of films	42
4.5.5	Optical properties of films	45
4.5.6	Swelling degree, solubility and moisture absorption	48
4.5.7	Packing of blackberries	50
5	Conclusions and future work	53
A	Appendix	55
	References	57

List of Figures

2.1	Biodegradation mechanism of bioplastics. Adapted from <i>Narrowing the gap for bioplastic use in food packaging-an update. Environmental Science & Technology</i> . by Zhao, X., Cornish, K., & Vodovotz, Y., 2020, <i>Environ. Sci. Technol.</i>	6
2.2	CPH harvesting and processing.	10
2.3	Chemical structures of chitin and chitosan.	12
2.4	Cellulose chemical structure.	13
3.1	Diagram of process of extraction of additives and preparation of chitosan-based films.	23
4.1	Pectin extraction from CPH.	26
4.2	FTIR spectrum of pectin enzymatically isolated of CPH.	27
4.3	Images of cellulose extraction process from CPH.	28
4.4	Contrast of FTIR spectra of cellulose extracted from CPH by (a) alkaline treatment and (b) enzymatic treatment.	29
4.5	XDR diffraction pattern of cellulose extracted from CPH by (a) alkaline treatment and (b) enzymatic treatment.	30
4.6	Appearance of the products obtained during the CNC production by enzymatic hydrolysis.	31
4.7	SEM microscopies of obtained CNC at (a) 80 μm , (b) 20 μm and (c) 10 μm , and SEM microscopies reported in the literature at (d) 100 μm , (e) 20 μm and (f) 4 μm	32
4.8	Contrast of FTIR spectra of a) cellulose and b) CNC.	33
4.9	XDR diffraction pattern of (a) cellulose and (b) CNC.	34
4.10	Dried DAC and DANC.	35
4.11	FTIR spectra of a) cellulose, b) DAC, c)CNC, and d) DANC.	36

4.12 XDR diffraction pattern of (a) cellulose and (b) DAC.	37
4.13 Photographs of chitosan-based films with different additives.	38
4.14 FTIR spectra of a) CH, b) CH/CNC/01, c) CH/CNC/02, and d) CNC.	40
4.15 FTIR spectra of a) CH, b) CH/DANC/01, c) CH/DANC/02, and d) DANC.	41
4.16 FTIR spectra of a) CH, b) CH/PCPH/01, c) CH/PCPH/02, d) CH/PCPH/05, and e) CH/PCPH/06.	42
4.17 SEM images of chitosan-based films. (a–c) Surface morphology of films. (d–f) Cross sections of films.	43
4.18 Mechanical properties of chitosan-based films made with different addi- tives concentrations. The percent above the column represents the amount of additive per film.	45
4.19 Optical transmittance (%T) of composite films.	47
4.20 Effect of chitosan-based films packing on quality and shelf life of black- berries.	51

List of Tables

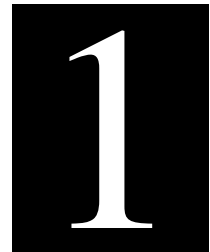
2.1	Types of bioplastics on the market.	6
2.2	Forms of biodegradable packaging.	9
2.3	Chemical composition of CPH.	10
2.4	Lignocellulose and pectin content in CPH.	10
2.5	Methods of extracting cellulose.	14
2.6	Standardize terms for cellulose nanomaterials.	15
3.1	Formulation of chitosan-based films.	20
4.1	Tensile measurements of chitosan-based films.	44
4.2	Swelling degree, solubility and moisture absorption of chitosan-based films.	48
A.1	Thickness of chitosan-based films.	55
A.2	Optical measures of chitosan-based films.	56

List of Symbols

Acronyms

$\% \epsilon$	Elongation at break	22
$\% \text{MA}$	Moisture absorption	22
$\% \text{WS}$	Water solubility	22
CH	Chitosan	2
CI	Cristallynity index	21
CNC	Cellulose nanocrystals	2
CPH	Cocoa pod husk	2
DANC	Dialdehyde nanocellulose	4
FTIR	Fourier-transform infrared spectroscopy	21
PCPH	Phenolic extract from CPH	4
SEM	Scanning electron microscopy	21
TS	Tensile strength	22
XDR	X-ray diffraction	21

Introduction



CHAPTER

In the Anthropocene era, plastics can be considered essential products with a wide range of uses being the engine of economic growth and comprehensive modernity. However, our high consumption and irresponsible disposal have made them the new challenge of the planet's sustainability. The COVID-19 pandemic has reemphasized the indispensable role of plastics in personal protector equipment, single-use medical equipment, and packing materials due to increased dependency on e-commerce because of the lockdowns, social distancing, and restrictions on public gathering.¹

Plastic materials started being used for packaging with plastic bags in the 1970s but increased their heavy use of disposable plastic packaging in food industry. The leading function of food packaging is to package food in a cost-effective way that meets industry demands and consumers by protecting the product it contains, preserving its safety and organoleptic characteristics.^{2,3} Several types of plastics are used for food packaging materials, including polyolefins, polyesters, polyvinyl chloride, polyvinylidene chloride, polystyrene, polyamides, and ethylene vinyl alcohols.³ These are petroleum-based products that tend to be single-use; being discarded easily and not degradable brings significant environmental issues. Traditional plastic food packaging solutions are generally a linear economy. Continued use of them leads to the depletion of non-renewable resources, greenhouse gas emissions during production and transportation, and solid waste generation.⁴ As a result, there is a critical need to develop and implement sustainable packaging solutions.

Biodegradable packages have been identified as a possible solution to this social and environmental challenge by reducing material usage, waste, and transportation costs. Several studies have been performed on the potential implementation of bio-based

materials, as biopolymers and their blends, in designing sustainable packaging materials that provide low cost, accessibility, biodegradability, and flexible processability.⁵ Biopolymers can be extracted from agro-waste, one of their most significant types; the polysaccharides, including cellulose and pectin, come from plants or animal sources like chitosan.⁶ Alone or into blends, these biopolymers offer attractive advantages: their renewable origin, non-toxicity and biocompatibility, average mechanical and barrier properties to water and gases.⁷

As promising materials, cellulose and chitosan (CH), the first and second-largest available biopolymers on Earth, have been studied for suitable applications in food packing. CH has unique biocompatible, biodegradable, mucoadhesion, and film-forming capabilities, as well as broad antibacterial activity,⁸⁻¹¹ making it a viable choice for the production of films for a wide range of packaging applications. However, by mixing CH with suitable reinforcing fillers, the mechanical and barrier characteristics of CH may be improved.⁸ Natural fillers have been widely used as reinforcing elements to replace synthetic or inorganic fillers in polymer matrices to produce bio-based nanocomposites. Cellulose-based fillers, such as cellulose nanocrystals (CNC), have structural, mechanical, and thermal properties¹² that allow the reinforcement of a polymeric matrix and the improvement of barrier, thermal, and mechanical properties.¹³⁻¹⁵ CNC/CH nanocomposite has been extensively studied among known CH-based composites in recent years.¹⁶⁻²⁶ Talebi et al.¹⁸ investigated the influence of CNC loading on the mechanical properties of CH-based nanocomposite films, finding that including 7% CNC in CH improved the biodegradable composite films' tensile performance by 104%. The natural antioxidant and antibacterial capabilities of CH-based films may be considerably increased by integrating different plant-based active components, extending the shelf life of perishable goods.^{10,27} Among others, it has been shown that black plum peel extract,²⁸ rosemary ethanol extract and essential oil,²⁹ Moringa oleifera leaves extract,³⁰ pomegranate peel extract,³¹ cranberry extract,³² grape seed and jaboticaba peel extract³³ can be used to accomplish this goal. In this regard, it has been reported that the Cocoa pod husk's (CPH) phenolic components contribute significantly to its antioxidant potential.³⁴

This research intends to investigate the effects of different CPH-based additives, blend ratios, plasticizers ratios, and preparation methods on the physical, mechanical properties, and functional performance of CH films and to compare the characterization of CH/CNC, CH/DNAC, and CH/PCPH films at different blend ratios. The capstone project report is structured in five chapters. In Chapter 1, general information about the context of the study is provided. Chapter 2 gives the theoretical background about our agro-waste material, the biopolymers involved, required characteristics for food packing applications, and extraction, blending, and film production methods. Chapter 3 describes

the experimental procedures listing CPH-based additives obtainment, film-forming, and characterization. In Chapter 4, results and discussions were summarized. Finally, Chapter 5 introduces the study's concluding remarks and future gaps.

1.1 Research context

Bioplastics that are 100% bio-based are now manufactured at a scale of 2 million tonnes per year and are being evaluated as part of future circular economies to accomplish some of the UN's Sustainable Development Goals.³⁵ The circular economy concept focuses on closing loops of material and energy flows and minimizing waste.³⁶ In this context, circular economy concerns can be addressed to the agroindustry, complementing the option of employing biopolymers synthesized from non-edible portions of plants or animals, reducing the risk of food depletion in local populations are in underdeveloped regions.³⁷ Commercial cacao production in Ecuador is a growing market with a forecast production of cocoa beans of 340 thousand tonnes for 2020/21.³⁸ On a year-on-year basis, cocoa beans from Ecuador in ICE Futures U.S. gradings increased from less than 1% to 14%.³⁹ However, the beans constitute only 33% of the fruit by weight, resulting in around two-thirds of the products as cocoa pod husk with minimal commercial value.⁴⁰ The chemical content of this pod includes fiber, phenols, carbohydrates, lignin, protein, and minerals that can be used to obtain biopolymers with biodegradable, bio-compostable, sustainable, and non-toxic characteristics.^{37,41} On the other hand regard CH, the seafood sector produces roughly 106 tons of waste each year, the majority of which is composted or turned into low-value-added goods like animal feed and fertilizers.⁴² From this waste, chitosan is obtained, which means that roughly 2000 tons of chitosan are generated yearly, with shrimp and crab shell remnants serving as the primary source of extraction.⁴³ Ecuador is one of the world's top shrimp producers and the largest in Latin America, with a feed market of 368,289 tons in 2020.⁴⁴ The market is expected to increase at a CAGR of 7.3 percent between 2021 and 2026, according to IMARC Group.⁴⁴ This study can overcome these problems by developing chitosan films with different additives extracted from cocoa pod husk. The films will be designed with chitosan to take advantage of the barrier and mechanical properties and modified with fillers, extracts, and pectin to enhance some of its properties.

1.2 Objectives

1.2.1 Main Objective

To develop biodegradable chitosan-based films incorporating CPH additives for their subsequent application in food packaging.

1.2.2 Specific Objectives

- To obtain crystalline cellulose from CPH through traditional and greener methods.
- To modify crystalline cellulose via size reduction and periodate oxidation.
- To use of cellulose nanocrystals (CNC), dialdehyde nanocellulose (DANC), and phenolic extract (PCPH) to improve chitosan biodegradable films' functional and mechanical properties.

Theoretical Frame Work



2.1 Food packing

Packaging is described as materials used to enclose or temporarily contain, handle, protect, or transport products and they are often discarded after use.⁴⁵ The essential functions of food packaging are to ensure food product preservation and safe conveyance till consumption, but also it offers needed information about the food.⁴⁶ Biologically, chemically, and physically, the quality of the food product might decline throughout distribution. Food packaging enhances the foods shelf life while maintaining quality and safety standards following government rules and policies.^{45,46} However, innovative packaging materials with enhanced characteristics and sensors that can monitor food quality have been added to food containers due to contemporary technology and materials science.⁴⁷

2.1.1 Biopacking

Any biodegradable packaging designed for long-term sustainability is called biopackaging or eco-conscious packaging. It uses biopolymers, which are natural and synthetic biodegradable polymers that can incorporate agro-industry by-products like fibers and inorganic or bioactive substances, to be more environmentally friendly.⁴⁵ PLA, cellulose, and starch are among the currently manufactured and used biopolymers in the market. There is, however, a distinction to be made between being biobased, biodegradable, and compostable. Biobased goods are made from renewable raw resources, whereas biodegradable products are made up of polymers that microorganisms may break down in the environment over time, including compostable bioplastics. As a result, all biodegradable bioplastics are compostable, but not all compostable bioplastics are biodegradable.⁴⁸ Table 2.1 lists the many types of bioplastics available on the market.

Table 2.1: Types of bioplastics on the market.

Types of bioplastic	Properties	Examples
Polymers from biomass	Compostable	Starch-based, cellulose-based, protein-based
Polymers from bio-derived monomers	Biodegradable or recyclable	PLA, bio-based PE, bio-based PET, bio-based PP
Polymers from microbial fermentation	Biodegradable	Polyhydroxyalkanoates (PHA)
Polymers from both bio-derived monomers and petroleum-based monomers	Biodegradable or recyclable	poly(butylene succinate) (PBS), poly(trimethylene terephthalate) (PTT), Pro-oxidant Additive Containing (PAC) plastic

Adapted from *Review of bioplastics as food packaging materials* by Hong, L., Yuhana, N., & Zawawi, E., 2021, *AIMS Materials Science*, 8(2), 166-184.

2.1.2 Biodegradation

The chemical process by which materials are metabolized into CO₂, water, and biomass by microorganisms' action is known as biodegradation. Figure 2.1 illustrates the biodegradation mechanism.⁴⁹ Commonly, the biodegradation process involves five steps:^{49,50}

1. *Biodeterioration*: The biodegradable material is superficially degraded and converted into tiny components by microbial species' joint action in the soil and other abiotic processes.
2. *Depolymerization*: Microorganisms secrete extracellular catalytic agents, mainly enzymes, that cleave the polymer chain into oligomers, dimers, and monomers.

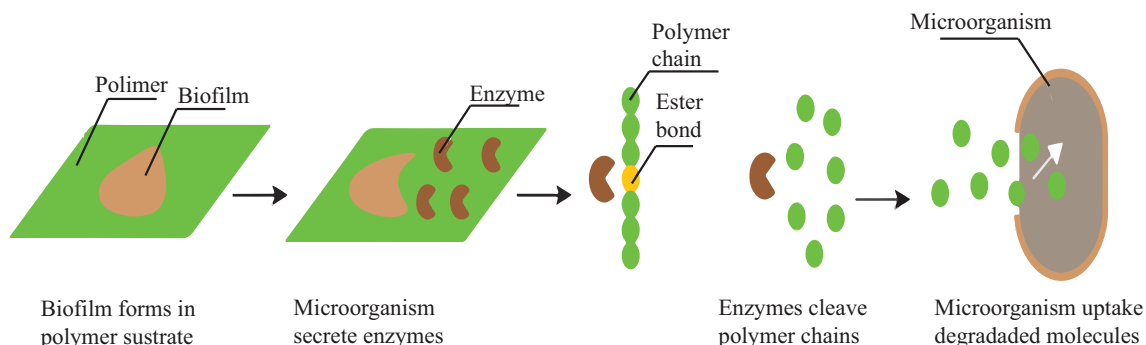


Figure 2.1: Biodegradation mechanism of bioplastics. Adapted from *Narrowing the gap for bioplastic use in food packaging-an update. Environmental Science & Technology.* by Zhao, X., Cornish, K., & Vodovotz, Y., 2020, *Environ. Sci. Technol.*

3. *Recognition*: Receptors of microbes recognize some fragmented oligomers, dimers, and monomers. They pass through the microbial cell's plasma membrane, leaving an unidentified component in the extracellular environment.
4. *Bioassimilation*: molecules in the cytoplasm are metabolized to primary and secondary metabolites.
5. *Mineralization*: the metabolites produced by the microbial cells are mineralized into CO₂, CH₄, H₂O, and other salts released in the environment.

The number and variety of polymer-degrading microorganisms vary depending on the environment, soil, sea, and compost, among other factors. The rate of degradation is influenced by the nature, type, position, and substrate type of the enzyme and environmental factors such as soil, pH, light, temperature, oxygen, and moisture. Furthermore, physical and chemical features of biopolymers, such as polymer chain length, crystallinity, and the complexity of the polymer formula, influence biodegradation. Polymers with shorter chains, weaker crystallinity, and simpler formulas are more susceptible to biodegradation.^{49,50}

2.1.3 Composting

Composting is accelerated aerobic biodegradation under managed environmental conditions like temperature, humidity, and present microorganisms.⁵⁰ It is an old technique for turning organic materials into fertile humus. Compost will be the top result of biodegradation of such organic waste, and water and carbon dioxide, which are already part of the biological carbon cycle, will not contribute to greenhouse gas emissions. Compositing benefits the soil by helping to retain moisture, increasing microbiological activity, enriching the soil with nutrients, and making it more breathable.⁴⁹

2.1.4 Packing properties

Biopolymers, if used alone, have poor tensile, mechanical, and barrier properties, which are responsible for their failure as solid and successful packaging materials. Thus, polymers are reinforced with nanofillers or crosslinked with others to improve their mechanical and barrier properties and impart novel characteristics.

Barrier properties

The bioplastic barrier properties are related to oxygen and other gases, moisture, and water permeability. The decreasing moisture/gas diffusion can be achieved by adding filler material. If the filler is impermeable to a gas or liquid diffusing into the polymer, the diffusing gas or liquid is forced to adopt a twisting path, lowering the permeability substantially.⁵¹ Very used fillers are nanoclays, nanocellulose, silica, silver nanoparticles, metal oxides, and carbon nanotubes.⁴⁵ Other methods used to enhance the barrier properties

include lamination with barrier plastics, which are primarily petroleum-based and non-biodegradable, and metallization, by vacuum coating aluminum oxide or silicon dioxide onto the plastics.⁵⁰

Mechanical properties

Bioplastics frequently experience brittleness and stiffness. Both external and internal, plasticization is a reasonably straightforward process for increasing polymer chain mobility, lowering the glass transition temperature, and improving flexibility.⁵⁰ On the other hand, internal plasticization is more efficient, yielding increased flexibility and strength while avoiding the plasticizer leaching that occurs with exterior plasticization. Blending with other polymers is the most popular strategy for improving polymer mechanical performance since it is a practical and cost-effective way to adjust polymer characteristics to their intended end-use.⁵² Bioplastic flexibility and toughness have also been improved via chemical copolymerization, grafting, and cross-linking.⁵⁰ Reinforcing fillers have also enhanced the mechanical properties of bioplastics, particularly strength and modulus.⁵¹

Thermal properties

The chemical structure, degree of crystallinity, and molecular weight of bioplastics influence their thermal stability. The thermal stability of polymers can be improved by chemical modifications such as adding aromatic structures to the polymer backbone, grafting, and cross-linking procedures. On the other hand, polymers are less resistant to high temperatures when they include double bonds or oxygen-containing structures in the main chain.⁴⁹ Other polymers and nanofillers, including nanocellulose, nanometal, nanoclay, and nanocarbon materials, can also improve thermal characteristics.⁵⁰

2.1.5 Forms of biodegradable packaging

Biobased materials have similar fundamental repeating chemical units as synthetic ones but demonstrate different chemical and physical properties. Processing and product development are not always cost-effective. Biopolymers' unique properties, such as biodegradability, make them attractive candidates that can replace conventional polymeric materials in different food packing forms, as summarized in Table 2.2.

Table 2.2: Forms of biodegradable packaging.

Forms	Description
Films	In every industry, films are the most extensively utilized form of bio-packaging. Biodegradable films were created to take the role of polyethylene film. Some essential characteristics of good packing films should include structural integrity, controlled respiration, suitable barrier properties, and prevention and reduction of microbial spoilage.
Containers	Thermoformed containers or trays can pack vegetables, salads, and fruits due to the regulated environment that is provided is essential to maintain the quality of such food goods.
Foamed product	Loose-fill molding, foam extrusion, expandable bead molding, and extrusion transfer molding are some of the processes used to make foamed items. Food packaging may be made from various products based on starch, such as trays and clamshells; however, direct food contact coatings are necessary.
Bags	Food goods may be stored and packaged using biodegradable bags, becoming the food sector its primary user. Biodegradable bags' raw material composition makes them flexible, sturdy, and resistant to breakage, moisture, and temperature change.
Gels	Hydrogels are biodegradable gels that are commonly used to avoid microbial infection. Complex hydrogels are a viable alternative to bio-based polymer synthesis. However, combining hydrogels from multiple polymeric materials reduces the shelf life of certain fruits, owing to water migration from the environment.

Adapted information from *An overview of biodegradable packaging in food industry* by Shaikh, S., Yaqoob, M., & Aggarwal, P., 2021, *Current Research in Food Science*, 4, 503–520.

2.2 Added value products from CPH

The cocoa plant (*Theobroma cacao*) is a member of the Sterculiaceae family that grows to 6–8 meters in tropical places.⁵³ CPH is obtained from cocoa processing Figure 2.2, and for every kilogram of cocoa bean received, ten times more CPH is created, being over 11 million tons of CPH annually worldwide.^{53,54} CPH has recently been evaluated for use in the culinary, cosmetic, pharmaceutical, and biomaterial sectors, based on their rich chemical and biological compositions.⁵⁵

2.2.1 Production and composition of CPH

The cocoa fruit major contains the cocoa beans embedded in the CPH, the primary by-product representing 56–79% of the total fruit weight.^{53,56} CPH is discarded after the cocoa de-podding, which removes the beans that are the valuable product.⁵³ CPH comprises three tissues named exocarp, mesocarp, and endocarp.^{57,58} The most common applications of the entire by-product are fertilizer or animal feed; however, its chemical composition allows using it for different purposes.⁵⁷ Table 2.3 reveals results in the literature for chemical

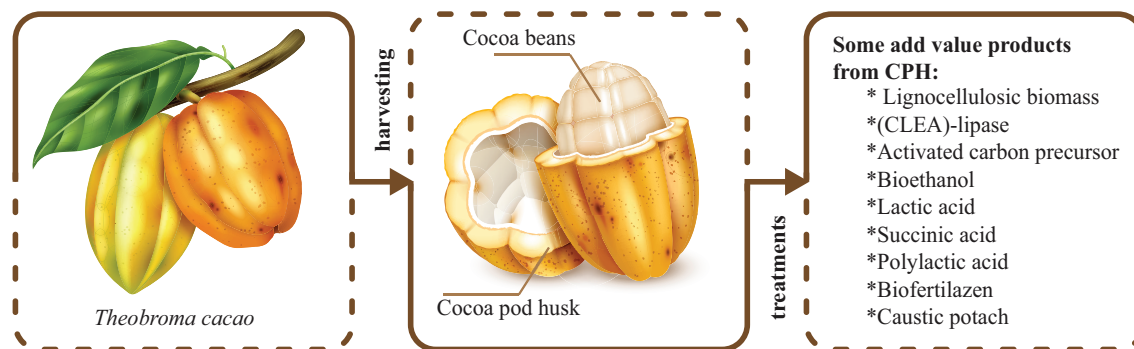


Figure 2.2: CPH harvesting and processing.

and composition analysis of the CPH. Before dryness, the moisture content is around 90%, but after, it is pretty low at about 10%.⁵³ It has been shown to contain a high fiber content of 32.1-35.0% and sugars 45% but lower crude protein content—5.0%–6.2%, crude fat—0.48-0.87%, and ash—8.76%.⁵⁷ Phytochemically contains more phenolic compounds (21%) than alkaloids (0.4 mg/100 g).⁵⁶ Table 2.4 shows the percent of the lignocellulosic components of CPH. Other compounds present in CPH are minerals such as Ca, K, P, Mg, Na, Zn, Fe, Cu, and Mn.^{58,59}

Table 2.3: Chemical composition of CPH.

Moisture (%)	Ash (g/100g)	Protein (g/100g)	Lipids (g/100g)	Carbohydrates (g/100g)	Reference
8.5	6.7	8.6	1.5	32.3	59
6.4-14.1	5.9-13.0	2.1-9.1	5.9-13.0	17.5-47	60
–	6.4-8.4	7-10	1.5-2	32-47	61
80.2	9.1	5.9	1.2	57.6	62
–	6.7-10.02	4.21-10.74	1.5-2.24	29.04-32.3	55

Table 2.4: Lignocellulose and pectin content in CPH.

Lignin(%)	Cellulose(%)	Hemicellulose(%)	Pectin(%)	Reference
14-28	19.7-26.1	8.7-12.8	6.12.6	61
14.7	35.4	37	–	63
23	33	37	3	56
14.6	24.24-35.0	8.72-11.0	6.7-9.2	55
38.42	44.69	11.15	10.1	64
38.8	35.3	6	–	60

2.2.2 CPH for the formulation of biocomposites

As exposed in the previous section, CPH is rich in minerals, lignocellulosic components, and antioxidants that allow it to be employed in many fields, including biocomposites' formulation. Using CPH as a reinforcing filler in biocomposites can save money while lowering environmental effects. However, the bonding strength between agricultural waste reinforcements and polymer matrices has to be improved. Coupling agents have been examined as one of the possible options. Chun et al.^{65,66} investigated the use of a palm oil-based coupling agent (POCA) in PP biocomposites using CPH as a filler, analyzing PP/CPH thermal characteristics and morphologies. The results revealed that a 3% POCA concentration provided the optimum tensile characteristics. When the agent content was less than 3%, the elongation at break reduced; however, it rose when the agent concentration was higher than 3%. Also, bioplastics from jackfruit seed starch have been reinforced with CPH fibers, demonstrating that by increasing the amount of CPH, the elongation at break value can decrease.⁶⁷ Furthermore, CPH lignocelluloses have been extracted and used as fillers for biocomposites. Lubis et al.⁶⁸ produced bioplastic from jackfruit seed starch reinforced with microcrystalline cellulose (MCC) extracted from CPH using glycerol as the plasticizer. MCC was obtained by alkaline treatment of CPH, bleaching, and hydrochloric acid hydrolysis, resulting in MCC with a rod-like shape and 74% crystallinity. The most promising composition resulted from starch to MCC mass ratio of 8:2, presenting a tensile strength of 0.637 MPa and elongation at a break of 7.04%. Azmin et al.⁶⁹ carried out the development of food packaging biofilms made of CPH-cellulose incorporated with sugarcane bagasse fiber. The most suited bioplastic comprises 75% cellulose and 25% fiber, displaying the lowest water absorption percentage and water vapor permeability, reducing the risk of mold formation and perhaps preventing moisture transfer between food and the environment. However, the resulting films exhibited brittleness and poor mechanical properties due to the hydrophilic nature of cellulose.

2.3 Chitosan

Chitin Figure 2.3a and chitosan Figure 2.3b are linear polysaccharides made of variable residual amounts of N-acetyl-2-amino-2-deoxy-D-glucose and 2-amino 2-deoxy-D-glucose linked to each other by β 1–4 glycosidic bonds.^{70,71}

2.3.1 Extraction process of chitin and chitosan

Chitin, the second most abundant biopolymer, is found in invertebrates, crustacean shells, insect cuticles, green algae, yeast, and the cell wall of fungi.^{71,72} Depending on these sources, the chitin exists in three polymeric forms: α - and β -, and γ -chitin, which corresponds to antiparallel, parallel, and alternating polymer chains, respectively.⁴³ Chitin's primary industrial source is crustacean shells containing 15–40% depending on the species,

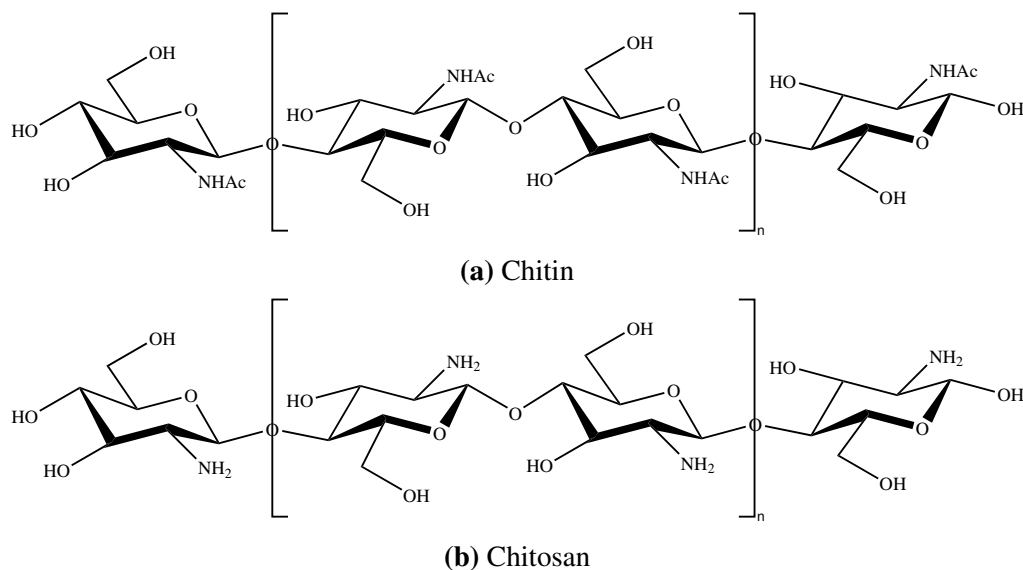


Figure 2.3: Chemical structures of chitin and chitosan.

with a maximum for shrimp shells.⁴³ Chemical extraction processes, enzymatic hydrolysis, biological/ microbial techniques, or their combination can be applied to extract chitin from the shell wastes.⁷³ The chemical procedure is commercially the most common method in chitin extraction techniques; however, it is environmentally unfriendly. As the shells contain 30–40% protein, 30–50% calcium carbonate and phosphate, the process involves eliminating them.⁷¹ The first step is demineralizing inorganic compounds using a diluted acidic medium as HCl solutions. The next step is the deproteinization employing an alkaline extraction commonly utilizing sodium hydroxide (NaOH) or potassium hydroxide (KOH) solutions.⁴³ If a colorless result is desired, a bleaching/decoloration phase is added as an extra step. Pigments like melanin and carotenoids are removed using an organic solvent like acetone or mild oxidizing treatments.⁴³ The most straightforward modification of chitin is N-deacetylation, which transforms it into chitosan by chemical, less often enzymatic, deacetylation reaction. Deacetylated chitin is commonly obtained using NaOH or KOH (40–50%) in a hardy alkaline hydrolysis procedure at high temperatures.⁷⁴ The reaction duration, temperature, concentration, and nature of the alkaline reagent are the essential factors in the deacetylation reaction and the source and isolation method of the original chitin.⁴³ Chitin is seldom completely N-deacetylated, and the differences between chitin and CH correlate to the degree of deacetylation (DD). According to the literature, the lowest DD, which corresponds to CH, ranges from 40 to 60%; however, most commercial samples have an average DD of 70–90%.⁷⁵ The DD and molecular weight greatly influence many physicochemical characteristics of chitosan, including solubility, hydrophilicity, crystallinity, and biological properties.⁷¹

2.3.2 Properties of chitosan

Chitosan is renowned for various unique features such as chelation, viscosity, and solubility in various vehicles, all impacted by diverse parameters such as DD, crystallinity, MW, and degrading techniques.⁷² Since its pKa value is roughly 6.5, the presence of substantial numbers of protonated $-NH_2$ groups on the chitosan structure allows for its solubility in acidic aqueous environments. When about half of all amino groups in chitosan are protonated, it becomes soluble. Chitosan is soluble in aqueous acetic acid solutions with a DD as low as 28%, and it is soluble in water with a DD of 49%.⁷⁶ As the molecular weight of chitosan is lowered, its viscosity drops. Shear viscosity rises as the chitosan DD rises, indicating that the sample with the greatest chitosan DD has seen more substantial chain expansion, resulting in a higher charge density in this sample.⁷⁶ Chitosan has chelating capabilities for various metal ions at an acidic pH. Chelation can occur on free amino groups (at near-neutral pH) or protonated amino groups through electrostatic attraction (acidic solutions).⁷² Chitosan is a non-toxic, biocompatible, and biodegradable polymer with also anti-inflammatory, anti-bacterial, anti-tumour, anti-fungal, haemostatic, and analgesic biological characteristics. Due to its cationic nature, chitosan has a powerful anti-bacterial and antifungal impact, allowing negatively charged lipids and proteins in the bacterial cell wall and negatively charged phospholipids in the cell membrane to interact.⁷²

2.4 Cellulose

Cellulose is a polysaccharide that consists of D-glucopyranose units linked via β -1,4 glycosidic bondsn Figure 2.4, forming a highly ordered molecular and supramolecular structure.⁷⁷ The cellulose macromolecule has four hydroxyl groups on one end and a carbonyl (aldehyde) group on the other, typically in the hemiacetal form. Cellulose hydroxyl groups are involved in intra- and intermolecular hydrogen bonds to a complex and highly ordered network with high crystallinity making it not soluble in water.⁷⁸ In this way, cellulose chains are assembled, alternating with crystalline and amorphous regions, forming the elementary fibril. These fibrils are grouped in a hemicellulose monolayer, encased in lignin and hemicellulose matrix, associated through physical interactions and covalent bonding.⁷⁹

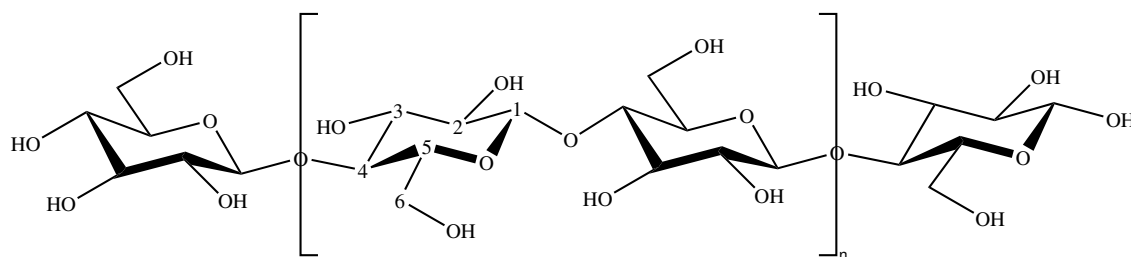


Figure 2.4: Cellulose chemical structure.

Table 2.5: Methods of extracting cellulose.

Method	Description
Alkaline Procedure	Plant tissues are digested with aqueous NaOH to remove lignin and hemicellulose. Bleaching and washing of the material may be involved in obtaining a higher purity material.
Ultrasound Treatment	The plant material is sequentially treated with water at 55 °C for 2 hours, irradiated with ultrasonic waves, and then treated with NaOH solutions.
Dilute Acid	Air-dried plant material is soaked in a 1% dilute sulfuric acid solution and heated to promote digestibility via lignin redistribution and hemicellulose dissolution.
Biological/Enzymatic treatment	Oxidoreductases can destroy unwanted lignocellulosic components like lignin. This technique uses peroxidases and laccases with high redox potential to directly oxidize or diffuse into the pores of the plant cell wall.

Adapted information from references^{82,83}

2.4.1 Extraction from agricultural waste

Cellulose may be obtained from various sources, including plants, algae, tunicates, and bacteria.⁸⁰ Lignocellulosic biomass or agricultural waste has 85–90% cellulose, hemicellulose, and lignin, which amount distribution varies depending on the source.⁸¹ The source of the material, chemical hydrolysis process, chemical concentration, time and temperature variations, type of pretreatment chemicals, and centrifugal force during mechanical processing all affect the characteristics of cellulose during extraction, according to different studies.⁸⁰ Table 2.5 describes the used methods to extract cellulose from plant tissues.

2.4.2 Nanocellulose

Nanoscale cellulose can be extracted from cellulose, capturing great attention due to its biodegradability, renewability, low density, and high mechanical properties.⁸⁴ It has a stiffness higher than Kevlar fiber, tensile strength higher than cast iron, and an eight-fold greater strength-to-weight ratio than stainless steel. Furthermore, nanocellulose is transparent and has many hydroxyl groups with reactive surfaces that may be functionalized to provide various surface features.⁸⁵ The word "nanocellulose" refers to a wide spectrum of nano- and micro-sized fibrils and crystalline particles. For the various types and forms, several terminologies have been utilized. Technical Association of the Pulp and Paper Industry (TAPPI) has developed a standard nomenclature for different sorts depending on their size and shape, summarized in Table 2.6.

Table 2.6: Standardize terms for cellulose nanomaterials.

Name	Abbreviation	Width	Length
Cellulose nanocrystal	CNC	(I) 3-10 nm (II) 3-20 nm	(II) 50-500 nm
Cellulose nanofibril	CNF	(I) 5-30 nm (II) 3-100 nm	(II) 0.5-2 μm
Cellulose microcrystal	CMC	(I) 10-15 μm (II) 10-50 μm	(II) 10-50 μm
Cellulose microfibril	CMF	(I) 10-100 nm (II) 10-100 nm	(I) 0.5-50 μm (II) 0.5-10's μm

Adapted from *Fabricating Sustainable All-Cellulose Composites* by Uusi-Tarkka, E., Skrifvars, M. & Haapala, A., 2021, *Appl. Sci.*, 11(21), 10069.

Applications

Nanocellulose is appealing for applications in many disciplines, including nanocomposite materials, surface modified materials, and translucent paper, due to its unique properties and biodegradability.⁸⁵ Nanocellulose has been chiefly used as a filler for polymeric matrixes in the food packing industry. Wang et al.⁸⁶ investigated the mechanical properties of synthetic polymers created by adding soybean nanocellulose and discovered that the tensile strength and stiffness of the nanocellulose-reinforced polymer are much higher than the pure base polymers. CNC may typically raise the strength and modulus of films up to an "optimum" CNC content, which is usually about 5%.⁸⁷ According to Fortunati et al.,⁸⁸ adding 3% CNC to polylactic acid films enhanced elastic modulus from 930 to 1050 MPa while maintaining transparency. Deng et al.⁸⁹ significantly decreased moisture loss and adhesion between layered foods by using CNF-chitosan film as food contact packaging applied to food with a very wet and sticky surface. Yu et al.⁹⁰ used CNF (60%), corn starch, and chitosan to make a biopolymer-based edible nanocomposite film that reduced the peroxide value of corn oil by 23% and improved antimicrobial properties. Cao et al.⁹¹ developed a pH-sensitive intelligent food packaging material by grafting hydroxy propyl triethyl-amine groups onto CNF and anchoring bromothymol blue. As the meat went from fresh to sub-fresh, the pale-yellow film became blue, suggesting that the intelligent film adequately represented the freshness of meat items. Nanocellulose may boost biopolymers' thermal, mechanical, and barrier properties and provide additional necessary functionalities to food packaging materials, such as antibacterial qualities, biosensor capabilities, and oxygen removal.⁷⁷

Experimental



CHAPTER

3.1 Reagents and Equipment

3.1.1 Biological material

Cocoa fruit was obtained from a cocoa Plantation of Quevedo, Los Rios Ecuador. Cellulase (enzyme activity 1,000 to 150,000 U/g) was provided by Carolina Biological Supply Company (Burlington, NC, USA).

3.1.2 Equipment

Cary 630 FTIR Spectrometer, X-ray diffractometer Mini-flex-600, UV/Vis/NIR LAMBDA 1050, SEM/EDS Phenom ProX, PHI 5000 Versa Probe III Scanning XPS Microprobe, SONOPLUS Bandelin ultrasonic homogenizer, PRO25D Homogenizer from PRO Scientific, Carver Hydraulic Unit Model #3912, Shel-Lab Vaccum Oven, Pol-Eko Oven Analytical Balance HR-150A from COBOS, 914 pH/Conductometer from Ω Metrohm, hot and stirrer Plate TOPO, Sorvall Legend XTR Centrifuge from Thermo Scientific, FreeZone lyophilizer, Leica DM4000 B LED microscope, DSTM 25 kN tester.

3.1.3 Materials and chemicals

Yachay Tech University and the project advisors provided all chemicals used in this study. Chitosan (ACS reagent grade, high molecular weight), sodium periodate (ACS reagent, $\geq 99.0\%$) and glycerol (ACS reagent, $\geq 99.5\%$) were obtained from Sigma-Aldrich. The other chemicals used herein were all analytical grades: citric acid anhydrous, absolute ethanol, sodium hydroxide, sodium chlorite, glacial acetic acid, sodium chloride. Distilled water was used in all reactions. Dialysis membrane (32 mm x 20.4 mm) was obtained from Innovating Science by ALDON Corporation. Petri dishes (Dia.90 mm x 16.5 mm, 1

room 4 vents) were provided by CITOTEST Labware Manufacturing CO.,LTD (Haimen, 226100 Jiangsu, P.R. China).

3.2 Sample preparation

The CPH was oven-dried at 40 °C for a week achieving complete dryness. First, a grain mill grounded dry CPH, and a hammer mill reduced it. The obtained material was separated using sieves mesh of 35, 60, 120, 230 and < 230 mesh. Every fraction was labeled and stored in PP plastic containers at room temperature.

3.3 Cellulose extraction

As explained next, two different pretreatment methodologies will carry out the cellulose extraction before the bleaching step. One uses the traditional approach (alkaline) and another a greener one (enzymatic).

3.3.1 Pretreatment

Alkaline leaching

The alkaline treatment for CPH followed experimental procedures reported elsewhere^{92,93} and the optimization process reported by Rochina⁹⁴ with modifications. In a 4 L beaker, 31.5 grams of 120 mesh CPH reacted with 3 liters of NaOH 4% solution under constant stirring at 80 °C for 3 hours. The resulting wine mixture was left to cool at room temperature and then separated and washed by multiple centrifugations to see a clearer mixture.

Enzymatic treatment: Pectin enzymatic extraction

The pectin enzymatic extraction was conducted using the procedure followed by Hennessey-Ramos et al.⁴¹ with some modifications. The commercially available cellulase carried out the enzymatic hydrolysis of CPH. In a 250 mL Kitasato flask, 10 grams of CPH, 200 mL of 50 mM citric acid buffer pH 4.6, and 0.7 grams of cellulase were placed. The top of the flask was sealed with a rubber tampon, and the sides were sealed with parafilm to prevent buffer evaporation and overpressure. The reaction was performed in an orbital shaker at 50 °C and 200 rpm for 20 hours. A fine-mesh strainer primarily filtered the resulting material, and the residues were squeezed using a cheesecloth. The obtained thick liquid was centrifuged at 4000 rpm for 5 min at 4 °C, and the supernatant was mixed with four times the volume of absolute ethanol. The material was refrigerated for two weeks; then, the formed gel was washed with twice the volume of 70% ethanol and cooled again for 2 hours. Then, it was centrifuged and dried in the fume hood. Once the obtained pectin dried utterly, the extraction yield was calculated, and the pectin remained refrigerated in methanol. The CPH residues after the filtration will be used for the bleaching step.

3.3.2 Bleaching

The same bleaching process was carried out for both pretreated samples, following the literature⁹³ with some changes. The resultant solid reacted with a solution of 2 liters of water, 12 mL of acetic acid, and 53 grams of sodium chlorite, which were added as 18 grams every hour. The reaction lasted 3 hours under conditions of 70 °C and constant stirring at 300 rpm. Then, the mixture was cooled and stayed under constant stirred for four days. The mixture was separated and washed by multiple centrifugations to obtain the cellulose slurry that was refrigerated. A small sample was stove dried to estimate the percent yield.

3.4 Cellulose size decreasing

The size reduction of cellulose followed the procedure reported by Zhai et al.⁹⁵ to obtain CNC by enzymatic method with some adaptations. The experimental setup is similar to the one described in section 3.3. In a Kitasato flask, 20 grams of cellulose slurry, 200 mL of 50 mM citric acid pH 4.6 buffer, and 0.47 grams of cellulase were added. The reaction was conducted in an orbital shaker at 50.8 °C and 200 rpm for 25.7 hours. After the reaction ran for the desired time, quenching it by cooling the flasks. The suspension was washed with 50 mL of distilled water and taken to an ultrasonic bath at 22 °C for 20 minutes. Then, it was centrifuged at 10000 rpm for 10 minutes. Some supernatant fluid was freeze-dried, and the rest refrigerated.

3.5 Cellulose oxidation

The size-reduced cellulose was oxidized to DANC by adapting the methodology found in the literature.^{96,97} 0.5 g of CNC, 0.76 g of sodium periodate, 0.49 g of sodium chloride, and 25 mL of distilled water were added to an Erlenmeyer flask covered by aluminum foil to prevent photoinduced decomposition of the periodate. The reaction was run in a water bath at 50 °C under magnetic stirring for 3 hours. The reaction ended with the addition of ethylene glycol. The product was filtered and dialyzed for four days until the conductivity was less than 50 $\mu S/cm$. The same procedure was done with the cellulose to obtain DAC.

3.6 Phenolic extraction

In an Erlenmeyer flask, 5 grams of < 60 mesh CPH were added with 100 mL of 80% ethanol for maceration. The flask was wrapped with aluminum foil and sealed with parafilm to stand in the darkness for 48 hours. The extract, PCPH, was filtered by gravity and stored in refrigeration.⁹⁸

Table 3.1: Formulation of chitosan-based films.

Additive	Formulation	Additive %	Glycerol %
	CH/C0		0
	CH/C2		2
	CH/C5		0.5
CNC	CH/CNC/01	5	0.5
	CH/CNC/02	3	0.5
DANC	CH/DANC/01	10	0.5
	CH/DANC/02	25	0.5
PCPH	CH/PCPH/01	0.25	0.5
	CH/PCPH/02	1	0.5
	CH/PCPH/03	0.25	2
	CH/PCPH/04	1	2
	CH/PCPH/05	5	0.5
	CH/PCPH/06	10	0.5

3.7 Films preparation

3.7.1 Chitosan and CNC nanocomposites

Films were prepared following commonly used protocols with minor changes.⁹⁹ 2% Chitosan forming-film suspension was prepared by dissolving chitosan powder in a 1 wt% acetic acid solution. The reaction lasted for 24 hours under constant stirring. Then, the mixture was centrifuged to degas and eliminate impurities. The chitosan matrix was homogenized with glycerol as a plastifier and CNC, following the formulations in Table 3.1. The casting weight was 25 ± 1 g into Petri dishes and dried under constant airflow in a fume hood.

3.7.2 Chitosan and DANC nonocomposites

Films were prepared according to the method reported by Gao et al.¹⁰⁰ with some variations. The chitosan suspension is the same described in section 3.8.1. The matrix suspension, the DANC, and the glycerol were homogenized in different proportions showed in Table 3.1, using the PRO25D apparatus at 10000 rpm for 5 minutes to disperse and degas fully. The film was weight cast, 25 ± 1 grams, and dried under constant airflow in a fume hood.

3.7.3 Chitosan and PCPH

The chitosan suspension is the same described in section 3.8.1. Several ratios of PCPH described in Table 3.1 were added to the chitosan matrix and blended at 800 rpm. The solution was degassed for 1 hour in an ultrasonic bath. The blends were cast over the Petri dishes with a casting weight of 25 ml and dried under constant airflow in a fume hood for 48 hours.¹⁰¹

3.8 Characterization

3.8.1 X-ray diffraction (XRD)

The XRD analysis for celluloses, CNC, and oxide cellulose was recorded with a Mini-flex-600 diffractometer (Rigaku, Akishima, Japan) with a D/tex Ultra 2 detector and a Ni-filtered Cu K α radiation ($\lambda = 0.15418$ nm). 40 kV and 15 mA were the operational voltage and current, respectively. At a scanning speed of 0.01°/s, the diffraction angle (2θ) was recorded from 5° to 60°. Before analysis, the samples were vacuum-dried. The Segal equation was used to calculate the crystallinity index (CI) of the samples:

$$CI\% = \frac{I_{002} - I_{AM}}{I_{002}} \quad (3.1)$$

where I_{002} corresponds to the intensity of the peak of the (002) plane ($I_{002}, 2\theta = 22.8^\circ$), and I_{AM} denotes the intensity of the amorphous halo ($I_{AM}, 2\theta = 18^\circ$).¹⁰²

3.8.2 Fourier-transform infrared spectroscopy (FTIR)

FTIR spectra of the extracted and synthesized samples and the resultant films were obtained using Cary 630 FTIR Spectrometer (Agilent, Santa Clara, CA, USA) and analyzed on OMNIC software, with spectral width ranging from 4000 to 400 cm^{-1} at the resolution of 4 cm^{-1} , and 64 scans per sample.

3.8.3 Scanning electron microscopy (SEM)

Morphology of CNC and microstructure of the surface and cross-section of the films was analyzed by a Phenon ProX Desktop Scanning Electron Microscopy (Thermo Scientific, Waltham, MA, USA). The CNC samples were cleaned with compressed air previous to each data collection and were examined with SEM at the accelerating voltage of 15 kV. The films were cut from cross-section imaging, cleaned with compressed air, and were analyzed with SEM at 5 kV.

3.8.4 Solubility

A vacuum-dry piece of film sized 1cm x 2cm was cut and then weighed to obtain the initial film dry weight. The water solubility of the films was tested by soaking them into a

25 mL beaker with 25 mL distilled water for 24 h at room temperature. The rest of the film was removed, dried, and weighed. Percentage water solubility was then calculated using the equation 3.2.

$$\%WS = \frac{W_{initial} - W_{final}}{W_{initial}} \times 100 \quad (3.2)$$

3.8.5 Moisture absorption

A vacuum-dry piece of films was cut and then weighed to obtain the initial film dry weight. The obtained pieces were placed in 10 mL beakers conditioned at room temperature in desiccators containing distilled water for one week. After the film pieces were removed, dried, and weighed, the moisture absorption was calculated using the equation 3.3.

$$\%MA = \frac{W_{final} - W_{initial}}{W_{initial}} \times 100 \quad (3.3)$$

3.8.6 Optical Transmittance Measurement

The optical transmittance of the films was measured using a LAMBDA 1050+ UV/Vis/NIR Spectrophotometer (PerkinElmer, Waltham, MA, USA) at a scanning speed of 50 nm s⁻¹ in the wavelength range of 250–800 nm. The transmittance of UV (280 nm) and visible (660 nm) areas was used to analyze the optical characteristics of pure chitosan and composite films.

3.8.7 Mechanical properties

Dumbbell-shaped type IV specimens were made by using a manual cutting press with a bent lever. Film thickness was examined using a digital micrometer at five random positions along with the specimen, and the average thickness was calculated. Tensile strength (TS) and elongation at break (% ϵ) tests were performed using a DSTM 10 kN tester (United Testing Systems, Fullerton, CA, USA) with an initial strain rate of 0.1 in./in.·min, an initial grip separation of 5 in., and a rate of grip separation of 0.5 in./min. The results were calculated based on at least two measurements.

3.8.8 Packaging of blackberries

Commercial blackberries were selected for this study by shape, size, and color, keeping the healthy ones. One blackberry was packed in every film, sealed with double phase tape trough all edges, and stored at room temperature for 17 days. Observations on the appearance change, weight loss, spoilage, and preservation of the fruit and the film were recorded.

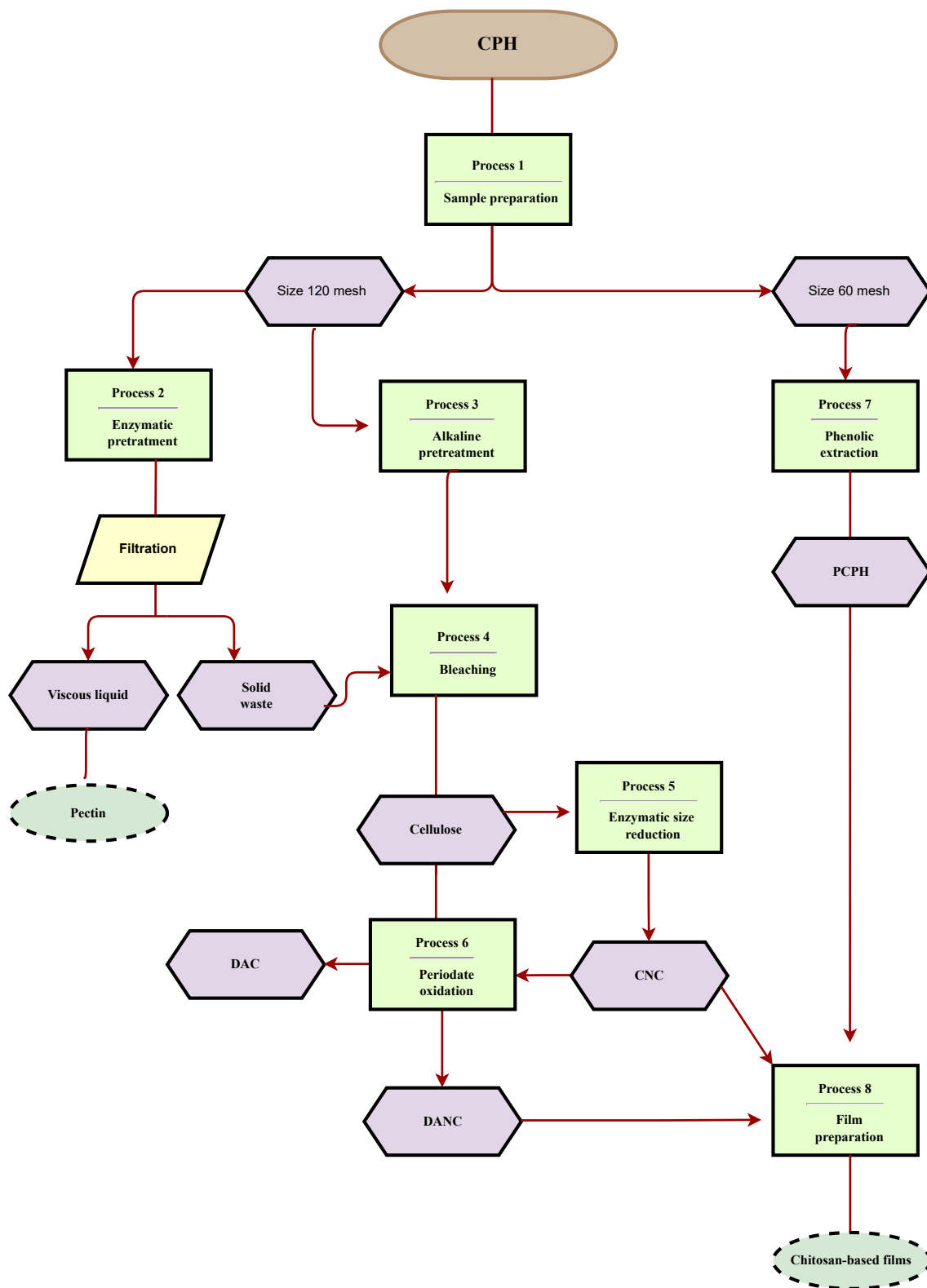
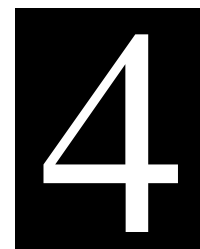


Figure 3.1: Diagram of process of extraction of additives and preparation of chitosan-based films.

Results



4.1 Pectin enzymatic extraction

CPH based pectin was extracted using cellulases under conditions previously reported.⁴¹ The usage of enzymes for pectin extraction might bring two practical approaches; the first is to use enzymes that degrade and isolate specific pectin fragments. Nevertheless, our approach is the second strategy consisting of enzymes that deconstruct the plant cell wall and isolate pectins.^{103,104} The plant cell wall is a supramolecular assemblage of polysaccharides such as hemicellulose, mainly xyloglucan.¹⁰⁵ The backbone of xyloglucan is made up of β -1,4-linked glucose units that are attached to cellulose microfibrils via hydrogen bonding.^{103,105} A pectic matrix and a protein network surround the cellulose/xyloglucan network. Cellulases are hydrolytic enzymes that degrade the cellulose/xyloglucan and protein networks to separate pectic polysaccharides by breaking β -1,4 glycosidic linkages between glucose units.⁷⁹ This kind extraction depends on the particle size of the CPH powder, the time, pH of the medium and temperature of the reaction, and the concentration of cellulases used.¹⁰⁶ The raw material must have a small particle size to enhance the contact surface and yield; hence the reaction was carried out with 120 mesh CPH. It was not used at a smaller one due to the complications of filtration in preliminary trials. Higher yields are found when harsher conditions are applied; then, the extraction was performed at pH 4.6, 20 hours, and 50 °C. The temperature was not higher because of the provider's suggestions to enhance the enzyme performance. The obtained viscous liquid after filtration has a brownish-orange color see Figure 4.1a. After two weeks of refrigeration, the color and viscosity did not change. When precipitated with pure ethanol, the gelification process was immediately seen Figure 4.1b. The air-dried pectin becomes darker and glowing on the surface, looking like candy Figure 4.1c. The percent yield for the pectin extraction of CPH was 12.02 %. Similar yields have been reported for the same

agro-waste, which varies between 6.46 % and 11.31 %.⁴¹



(a) Viscous liquid after filtration. (b) Precipitation with ethanol. (c) Dried pectin.

Figure 4.1: Pectin extraction from CPH.

Extracted pectin was characterized using FTIR as proof for its chemical structure. Figure 4.2 shows the pectin spectrum with its characteristic peaks. A broad peak at 3310 cm^{-1} corresponds to the stretching vibration of -OH groups of carboxylic acid and alcohol. The peak at 2932 cm^{-1} corresponds to the stretching vibration of C-H groups of methyl. An esterified carboxyl group's distinctive stretching vibration band (COOR) is at 1740 cm^{-1} , the asymmetrical stretching of the carboxylate ion (COO⁻) at 1633 cm^{-1} and symmetric stretching band at 1440 cm^{-1} . In the 'fingerprint' region, the bands between $1120\text{--}990\text{ cm}^{-1}$ allow spectral identification of galacturonic acid in pectin molecules.¹⁰⁷ The peak at 1013 cm^{-1} indicated that the CPH pectin sample contains pyranose, while the peaks at 920 cm^{-1} and 830 cm^{-1} indicated absorption of dglucopyranosyl and α -d-mannopyranose, respectively; similar findings were reported for apple pectin in previous studies by Wang et al.,¹⁰⁸ Zhang et al.¹⁰⁹ and Dranca et al.¹⁰⁴

4.2 Cellulose extraction

Cellulose was obtained from CPH utilizing two methodologies: the conventional approach using an alkaline pretreatment and the greener approach using an enzymatic one. As previously mentioned, the cell wall is constructed by several polysaccharides, including cellulose. Then, to extract cellulose is necessary to disrupt their assemblage and remove them. The alkaline pretreatment is primarily a delignification process based on solvation and saponification, which results in depolymerization and cleavage of the ester linkages that crosslink lignin and hemicellulose.¹¹⁰ Alkaline hydrolysis causes the interfibrillar areas to separate from the cellulose fibers by disrupting OH bonding in the fiber network structure by ionizing the hydroxyl groups of different components in the fibers to produce alkoxide. Even so, the separated cementing materials would be treated to alkali dissolving in order to separate the bundles of cellulose fibrils while lowering the cellulose fibers

dimension.¹¹⁰ During this treatment, the lignin release is evident because of the color change to a dark purple solution (Figure 4.3a) similar to that reported by Zhang et al.¹¹¹ and Kininge et al.¹¹² The resulted mixture was washed multiple times accompanied by centrifugation. As a lower pH was achieved, the coloration became lighter. Probably this is the least favorable step of this procedure because of the sizeable alkaline waste. It turned to clean chemical processes for obtaining cellulose as enzymatic hydrolysis in response to these issues. As exposed in Figure 3.1, cellulase breaks the β -1,4 glycosidic bonds to obtain pectin. However, cellulase also modifies and degrades the lignin and hemicellulose by limiting the degree of hydrolysis or selectively hydrolyzing specific components in cellulosic fibers.¹¹³ The de-pectinated CPH (Figure 4.3b) is enriched in cellulose fibers after pectin extraction. A bleaching step using sodium chlorite (NaClO_2) was performed in both approaches to complete the extraction process. This bleaching agent was chosen because of its high solubility in water and capacity to keep product strength due to its low oxidation potential compared to other bleaching agents.¹¹⁴ Sodium chlorite was utilized in an acid medium where metastable chlorous acid (HClO_2) is degraded to chlorite (ClO_2^-), which is subsequently oxidized to chlorate (ClO_3^-). After that, chlorine dioxide (ClO_2) and chloride are produced (Cl^-). The sodium chlorite then creates an oxidative solution, including oxychloro species as a consequence.¹¹⁴ The remaining lignin is oxidized in

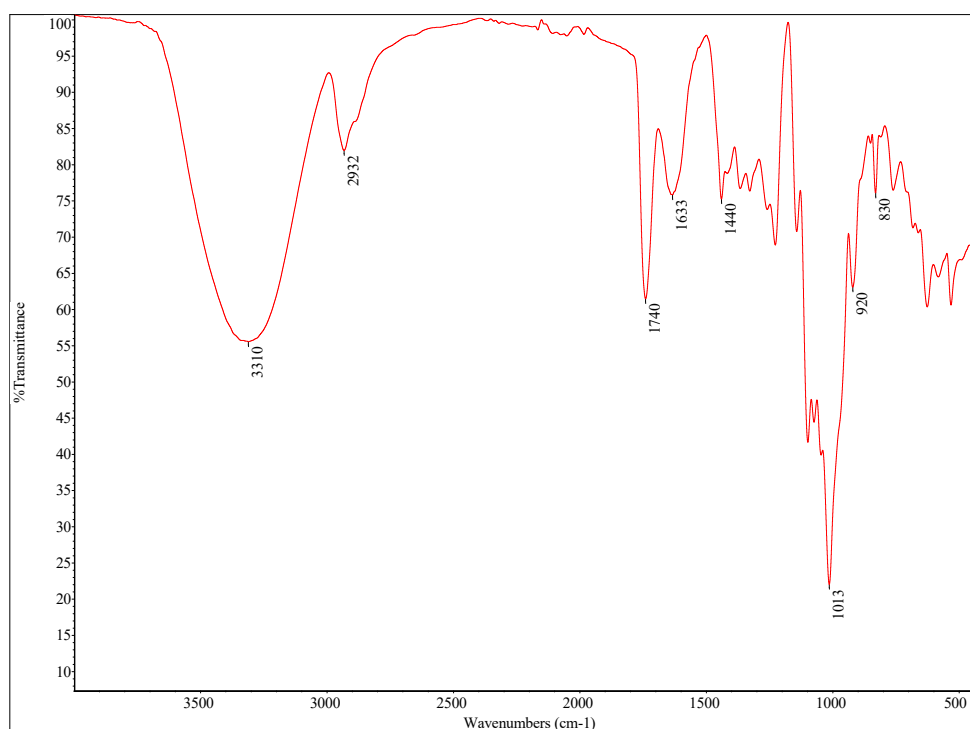
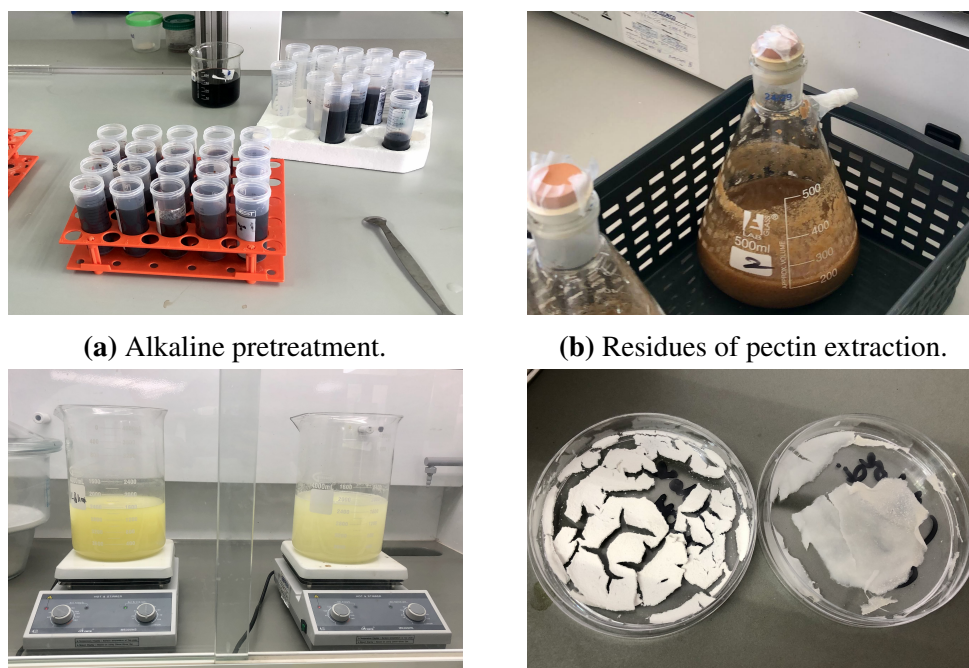


Figure 4.2: FTIR spectrum of pectin enzymatically isolated of CPH.



(a) Alkaline pretreatment. (b) Residues of pectin extraction. (c) Bleaching step for alkaline (left) and enzymatic (right) pretreatments. (d) Dried alkaline treated (left) and enzymatic treated (right) cellulose.

Figure 4.3: Images of cellulose extraction process from CPH.

this step. It was evident because of the color change of the solution to a bright yellow. The colorations were slightly different, which could be caused by the difference in the lignin percent leftover by the pretreatment Figure 4.3c. In a study by Bacci et al.,¹¹⁵ different methods, including chemical and enzymatic, were employed to extract cellulose from nettle stalks, resulting in higher content of cellulose fibers with lower lignin and hemicellulose content for the alkaline one. It corresponds with the estimated yields for the two methods. In the alkaline one, the estimated percent yield was 38%, while the enzymatic one was 20%.

The dried cellulose materials showed different appearances; the caustic one was more white and dried as cardboard (Figure 4.3d, left). The another one was yellowish and dried as thin sheets with heterogeneous particle distribution (Figure 4.3d, right). From this first sign, it is notorious that the two resultant cellulose are not the same by possible variations in the chemical composition and crystallinity. Therefore, FT-IR and XDR results were compared to identify their differences.

Figure 4.4 presents the FT-IR spectra from both samples exhibiting two distinctive absorbance regions, the first one from 3500 to 2700 cm^{-1} and the second one from 1800 to 600 cm^{-1} . For the cellulose obtained for alkaline treatment, Figure 4.4a shows a broad peak located at 3329 and 3291 cm^{-1} assigned to inter- and intramolecular hydrogen bonding ($-\text{OH}$) stretching vibrations, respectively.¹¹⁶ The band around 2912 cm^{-1} is associated with C-H stretching vibrations of methyl, methylene, and methine

groups.^{117,118} Similar bands to previously explained are reported for enzymatic extracted cellulose Figure 4.4b. The variation of the products is evident in the second region.

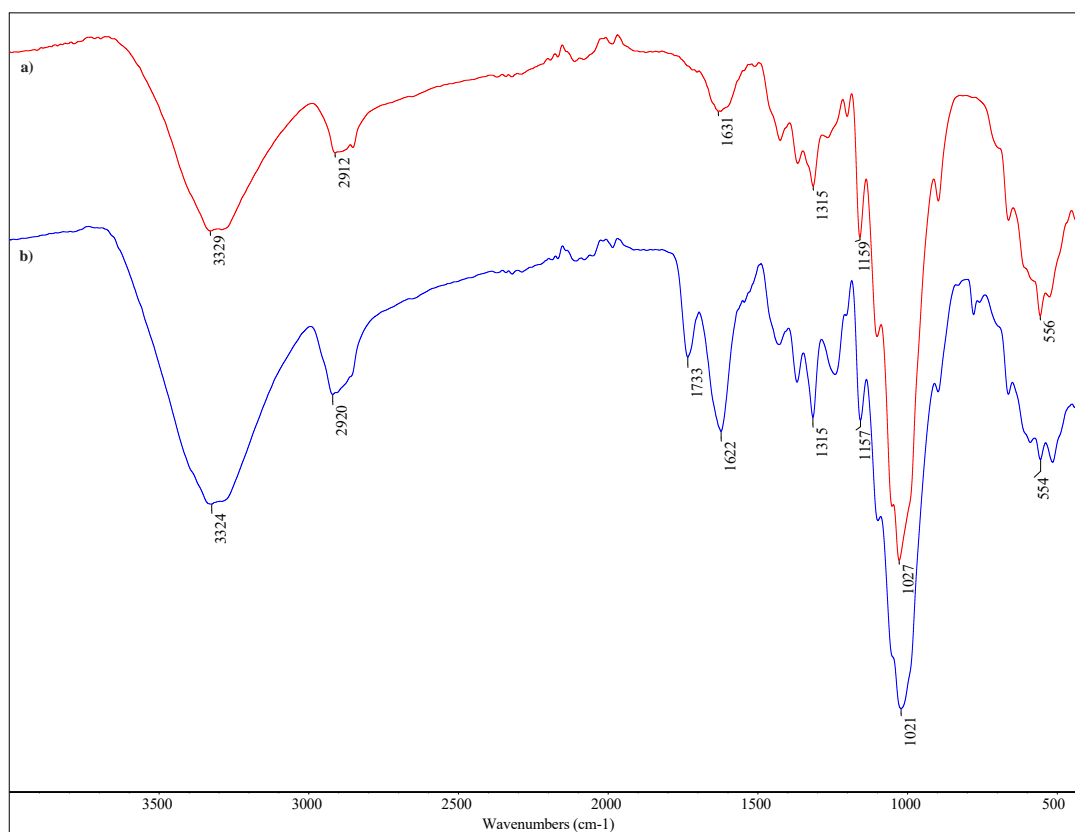


Figure 4.4: Contrast of FTIR spectra of cellulose extracted from CPH by (a) alkaline treatment and (b) enzymatic treatment.

The similar peaks at this region are associated with the $\text{CH}_2\text{-O-H}$ bending or H-O-H bending vibration of absorbed water located at 1631 and 1622 cm^{-1} ,¹¹⁶ and the strongest one assigned to the stretching vibration of C-OH of primary alcohols at 1027 and 1021 cm^{-1} .^{119,120} The critical difference between the two spectra is the peak at 1733 cm^{-1} , which corresponds to the stretching vibration C=O of the carboxyl group of the glucuronic acid (GlcA) unit and is only present in the enzymatic one. This band is typical of hemicelluloses, as well as the C-O stretching band at 1241 cm^{-1} as was reported by Cheng et al.¹²¹ Based on this data, we may presume that the enzymatically extracted product is holocellulose, which is made up of cellulose and hemicellulose. This holocellulose has unique features by preserving the structure and high content of the hygroscopic and amorphous hemicellulose phase.¹²² This can imply a decrease in crystallinity. The peak at 1425 cm^{-1} corresponds to asymmetric $-\text{CH}_2$ wagging, which becomes broader while decreasing crystallinity as the case of 4.4b at 1428 cm^{-1} .^{116,119} Also, the decrease of crystallinity can be seen by considering the intensity decrease of the peaks corresponding to the anti-symmetric bridge C1-O-C4 stretching and the anti-symmetric in-plane ring

stretching vibration at 1159 and 1101 cm^{-1} , respectively.¹²⁰ The peak at 897 cm^{-1} is known as the amorphous absorption band, being the CO-C stretching at β -(1-4)-glycosidic linkage, here the cellulose crystallinity decreases as the relative intensity of the amorphous band increases.¹¹⁶

The extracted products were analyzed by XRD, and the obtained diffractograms are shown in Figure 4.5. The three characteristic peaks for cellulose were displayed in both materials spectra. In the case of the cellulose, $2\theta = 16^\circ$, 22.7° and 35° , relating to the (110), (200), and (004) crystal planes of the cellulose I polymorph respectively.^{117,118} The more intense peak was observed at 22.7° , confirming the presence of crystalline cellulose. The CI for this sample was 74.9%. Similar CI was reported for CPH⁹³ (63.3%), agave¹¹⁸ (74%), celluloses of jack fruit¹¹⁷ (83.42%), and sugar cane bagasse¹¹² (46.59%). For the holocellulose, the same lattice planes were found at $2\theta = 15.7^\circ$, 22° , and 34.9° . The CI for this sample was 60.2%, slightly lower to the result reported by Hassan et al.¹²³ ($\sim 71\%$). The data clearly shows that the crystallinity of the isolated materials increases with the harshest treatment due to the removal of the amorphous constituents and the rearrangement of the crystalline regions into a more ordered structure.¹¹⁸

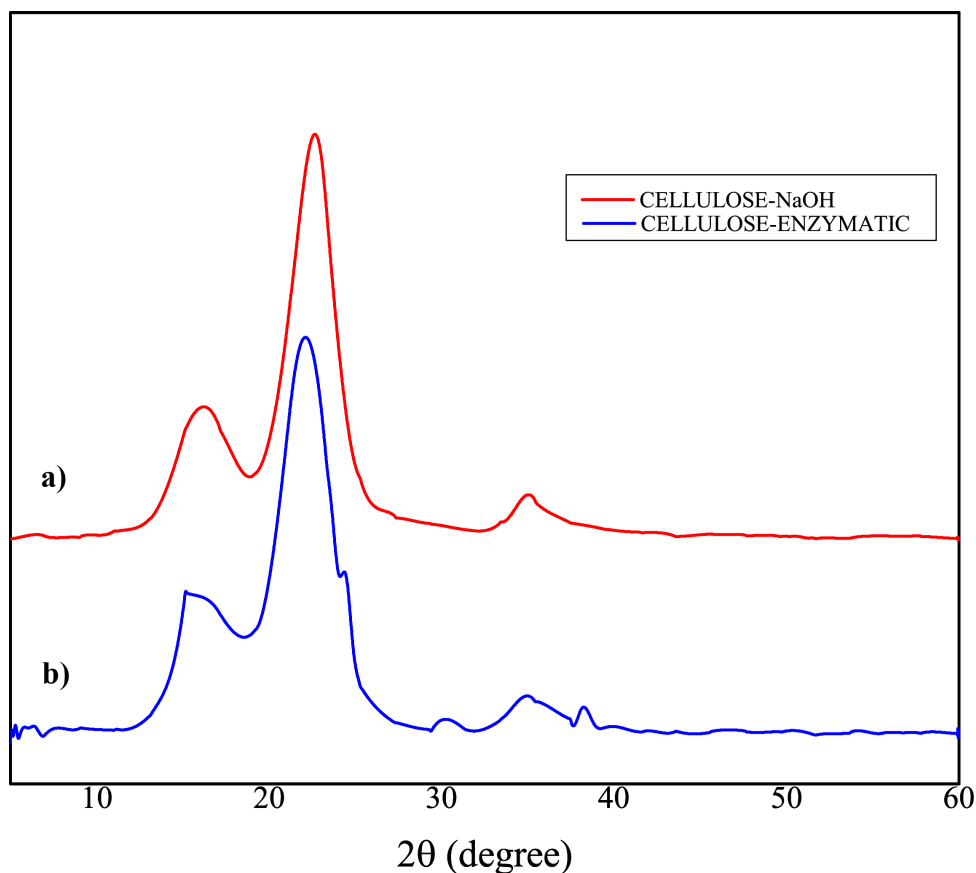


Figure 4.5: XRD diffraction pattern of cellulose extracted from CPH by (a) alkaline treatment and (b) enzymatic treatment.

4.3 Cellulose size decreasing: CNC

Highly ordered crystalline areas are intermingled with disorganized or amorphous regions in cellulose. Because the cellulose chains are more accessible in amorphous areas than in crystalline sections, they are more prone to enzymatic breakdown.⁹⁵ Cellulase may hydrolyze the amorphous portion of the cell wall while leaving the crystalline portion intact.¹²⁴ In this case, CNC was obtained via cellulase hydrolysis Figure 4.6a, which reduces pollution caused by other procedures. However, strict hydrolysis conditions are necessary to sustain enzyme activity during the enzymatic hydrolysis process.¹²⁵ Factors such as temperature, pH, rotation speed, enzyme loading, and time regulate this process.¹²⁶ The temperature of this hydrolysis was set at 50.8 °C, as advised by Zhai et al.,⁹⁵ since higher temperatures might reduce the activation energy of CPH cellulose molecules, speeding up molecular collisions between enzyme and cellulose and boosting reaction rate. However, the process should not exceed the enzyme's ideal temperature since this would slow down the catalytic reaction rate. In addition, Zhang et al.¹²⁶ reported that lowering sugar content does not significantly increase in temperature ranges around 50 °C. pH impacts the dissociation behavior of the substrate as well as the spatial organization and dissociation state of active groups in the enzyme, making it one of the most important parameters determining enzyme-catalyzed activities.¹²⁷ The pH of the hydrolysis was 4.6 due to the favorable dissociation degree of the functional groups of the enzyme activity center and cellulose molecule.⁹⁵ The remaining buffer can be further fermented into ethanol and other bioproducts from this reaction, providing significant additional value for the CPH production line.¹²⁶ The rotation speed was set up at 200 rpm to promote the contact possibility between the enzyme and the substrate; however, it could also decrease mass transfer limitation.¹²⁶ Variations in this parameter should be explored to identify an optimal one. CNCs preparation used an enzyme loading of about 1430 U/g. Calculating the particular load was challenging because of the provider's large unit per gram disparity.

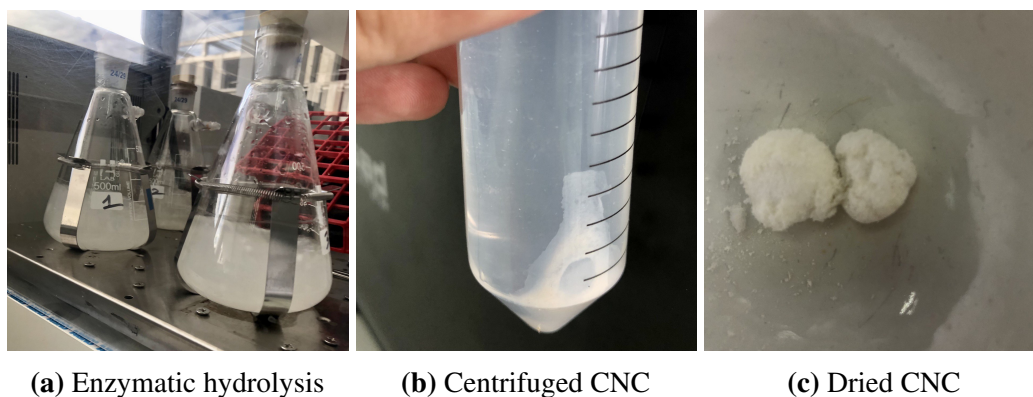


Figure 4.6: Appearance of the products obtained during the CNC production by enzymatic hydrolysis.

By increasing the binding sites, an increase in enzyme load tends to boost yield. On the other hand, larger loads may cause CNCs to be further hydrolyzed to sugars due to the saturation of the active site on the cellulose, according to Boonsombuti et al.¹²⁸ It is vital to identify cellulose type before determining the extraction time because the conversion rate varies based on it. The obtained cellulose was classed as type I in the preceding section. It has been reported that enzymatic hydrolysis rate is faster for cellulose II than I because of the differences in cellular chains disposition that affects the partial cleavage of hydrogen bonds in water and the hydrophobic interactions.¹²⁹ As a result, extended extraction times should be taken into account. Zhang et al.¹²⁶ proposed that optimal times of CNC production was 48 h due to the yield rising progressively when the milling time was increased. However, according to Zhai's⁹⁵ findings, an extraction duration of fewer than 30 hours was sufficient to preserve cellulose characteristics and was unlikely to deteriorate. The hydrolysis time was 25.7 h because the available equipment does not have humidity control; hence more significant times would mean losing all the medium.

The evolution of the enzymatic hydrolysis involved changes in turbidity. Firstly, the mixture was dense white slurry while at the end resulted in some cleared one, which has been explained as one of the effects of the size reduction of the cellulose.¹³⁰ After centrifugation, a white aggregate could be visualized in the bottom, but some particles remained in the supernatant Figure 4.6b. The resulting cellulose was white and looked like a sponge after the drying process Figure 4.6c.

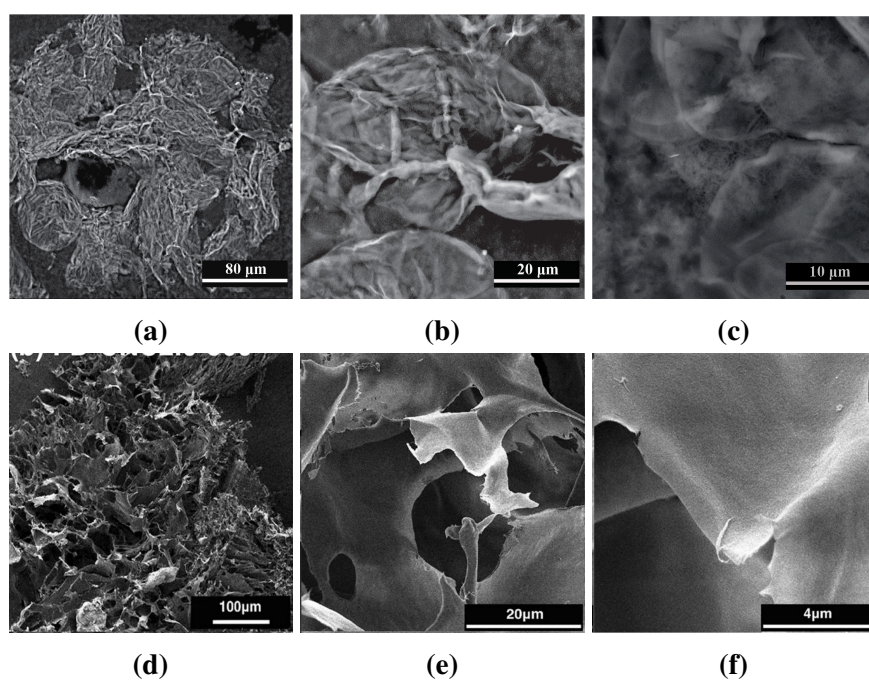


Figure 4.7: SEM microscopies of obtained CNC at (a) 80 μm, (b) 20 μm and (c) 10 μm, and SEM microscopies reported in the literature at (d) 100 μm, (e) 20 μm and (f) 4 μm.

CNC's microscopic morphology(a-c) is depicted at a different scale in SEM micrographs in Figure 4.7. The CNC exhibits porous and large irregularly shaped flakes of various sizes Figure 4.7a. The influence of the drying process in CNC morphology was investigated by Abdallah et al.¹³¹ The resulting CNC was dried using freeze-drying equipment, with the aggregation process determined by ice formation and growth rate. As a result of the ice formation, CNC particles collide and aggregate, resulting in bigger flakes, as seen in Figure 4.7c. The obtained micrographs are in agreement with those previously reported (d-f) where the dried method was evaluated to obtained the different forms of CNC.¹³¹

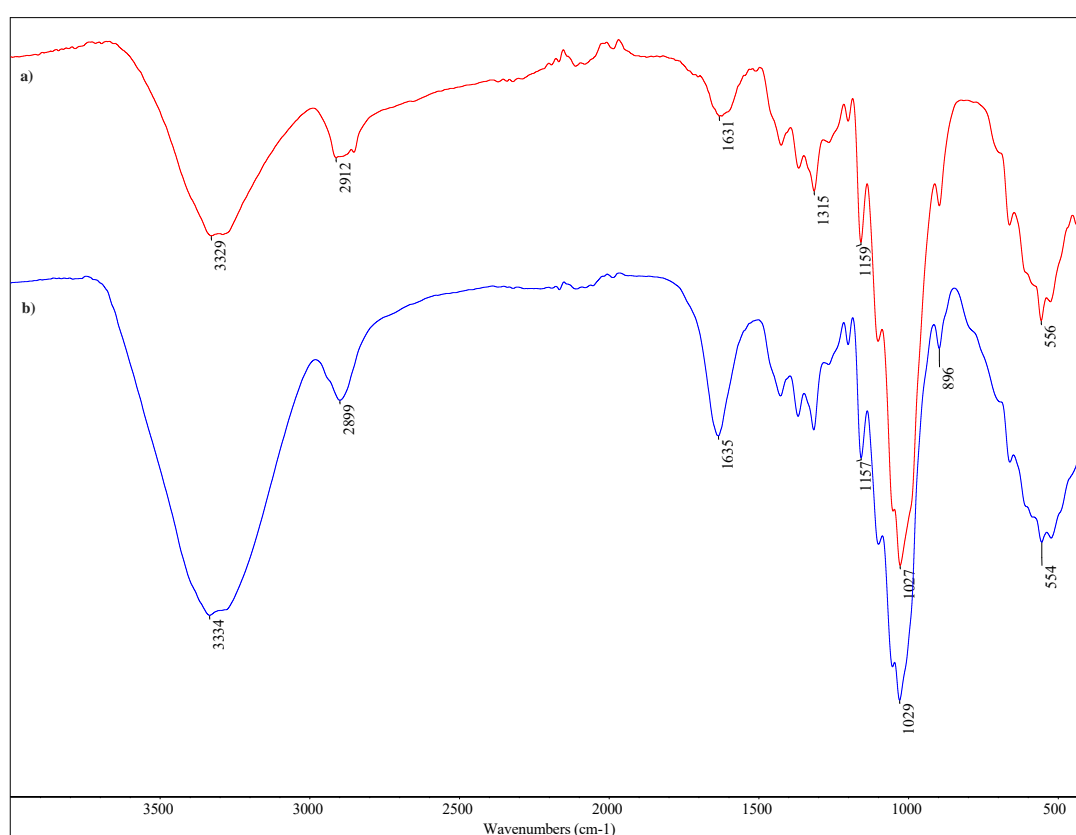


Figure 4.8: Contrast of FTIR spectra of a) cellulose and b) CNC.

The possible changes in the chemical structure of the extracted cellulose and CNC were evaluated by FTIR. As shown in Figure 4.8, both spectra showed the same absorption peaks around 3330, 2900, 1631, 1029, and 896 cm^{-1} and can be explained precisely as in the previous section. A significant band occurred at roughly 3300 cm^{-1} for cellulose and CNCs samples, related to hydroxyl groups' stretching vibration. The peak in CNC was more prominent than in the regular cellulose, indicating an increase in the hydroxyl groups (-OH) of cellulose. This result corresponds with the intensity of the peak associated with the bending vibration of the water molecule. Compared with the regular one, the peak

intensity increased in the spectrum of CNC, which indicated that CNC had absorbed more water molecules. It also can be associated with the drying method. The literature suggests 48 straight hours of drying, but because of the availability of equipment, CNC was dried for only 24 h. From both FTIR spectra, one can see that there was no noticeable difference in chemical structures between the two samples.

Figure 4.9 shows the XRD patterns of both samples. For CNC is distinguished three significant peaks at $2\theta = 15.9^\circ$, 22.2° , and 35.3° , which correlate to crystallographic planes (110), (200), and (004), respectively.^{117,118} These peaks are identical to the cellulose peaks ($2\theta = 16^\circ$, 22.7° , and 35°). CNC is also classed as cellulose I structure, which indicates that following enzymatic hydrolysis the CNC retains its original crystalline structure. The CI of the produced CNCs reduced somewhat from 74.9% to 70.5% percent, likely due to physical destruction, which resulted in crystalline order rearrangement in the (004) plane or some degradation to reducing sugars.¹³²

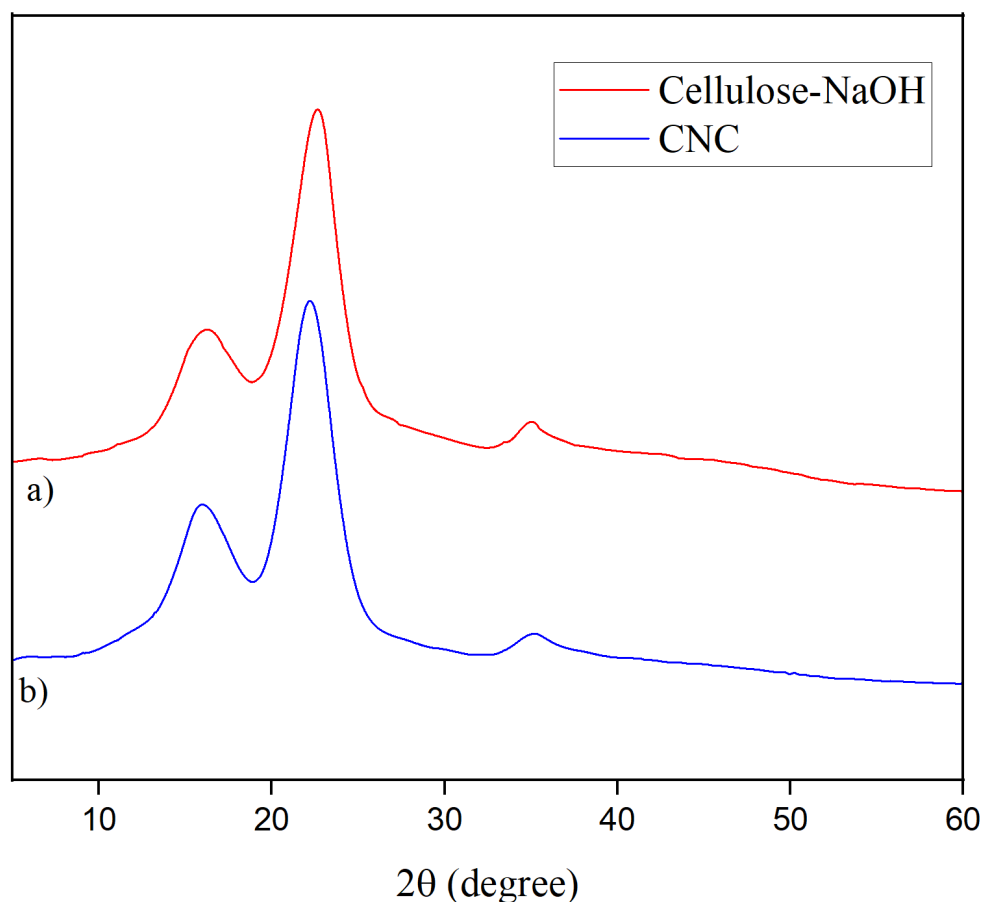


Figure 4.9: XDR diffraction pattern of (a) cellulose and (b) CNC.

4.4 Cellulose Oxidation

The dialdehyde cellulose and DANC can be synthesized by using sodium periodate oxidation in the selective oxidative cleavage of the bonds between the C2 and C3 of the anhydroglucopyranose unit, whereas the C6 atom remains unoxidized.^{96,133} Under the same conditions, the undesired degradation reaction by oxidative/hydrolytic cleavages of glycoside bonds can also occur.¹³⁴ Previous research has shown that pH, periodate dosage, and temperature are conditional factors in preparing oxidized cellulose by periodate oxidation.¹³⁵ Sirviö et al.¹³³ demonstrated that metallic salts and an elevated temperature could accelerate the oxidation reaction; thus, a higher aldehyde content can be achieved compared to an oxidation process at room temperature without adding salts. The reactions on the fiber's surface are classed as solid-liquid heterogeneous reactions that depend on the active parts on the surface of cellulose and the medium acidity.¹³⁴ Therefore, it has been established that a lower pH accompanied a higher aldehyde group content but a lower yield because of the decreased acidic/oxidative cleavages of glucosidic bonds.⁹⁶ The reaction was carried out in acidic media with a pH near 2 to promote aldehyde content. In this work, an AGU/periodate molar ratio of 1 to 1 was used as suggested by Wang et al.⁹⁷ based on that the oxidation reaction rate may enhance with a higher concentration of periodate. The optimal temperature for the reaction has been studied relatively in literature^{96,97,134} where 45 °C was suggested. However, Sirviö¹³³ indicated that at temperatures around 75 °C in just three hours, DAC may achieve six times higher aldehyde contents than the corresponding oxidation at room temperature. The temperature herein was set up around 50°C for 3 hours to prevent the sodium periodate decomposition, iodine production, and DAC degradation that are more likely to occur at higher temperatures.⁹⁶ The obtained oxidated samples presented different appearances after being freeze-dried. The DAC remained white and formed cardboard after being in a hydraulic press Figure 4.10a. Nevertheless, the DANC becomes darker and a powder Figure 4.10b. These differences

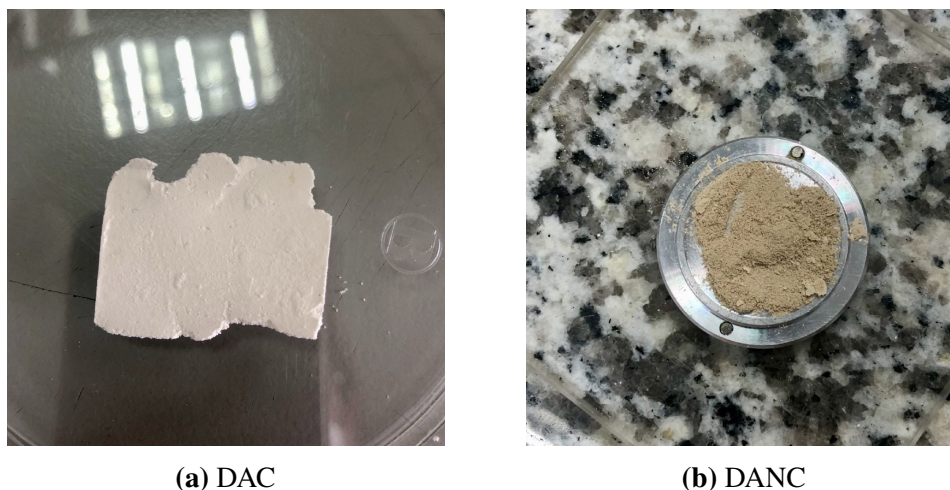


Figure 4.10: Dried DAC and DANC.

indicate that the particle size affects the methodology for periodate oxidation. Then, the appearance variation can be attributed to a different chemical composition that the FTIR analysis will corroborate.

Figure 4.11 presents the FTIR spectra of cellulose, DAC, CNC, and DANC. The main peaks in all samples can be assigned as: at 3334–3305 cm^{-1} for the stretching of hydroxyl groups, at 2920–2885 cm^{-1} for the C–H vibrations, at near 1630 cm^{-1} due to the absorbed moisture of the samples, between 1030 cm^{-1} and 1160 cm^{-1} are assigned to the C–O stretching.¹³⁴ Compared to unmodified cellulose and CNC, the characteristic absorption band of C=O stretching of aldehydes is 1722 cm^{-1} for DAC and DANC being relatively weak due to the formation of the hemiacetal linkage structure between aldehyde and hydroxyl groups of AGU during the preparation.^{96,135} The peak at 1632 cm^{-1} in the DANC sample is too high, which suggests that the sample was oxidized until carboxylate formation, making it useful as intermediates in cellulose-based functional products such drug carriers and heavy metal adsorbents.⁹⁶ A slight redshift of the hemiacetal vibration peak at 896 cm^{-1} implies a skeletal change on the main chain of cellulose and CNC.¹³⁴ Furthermore, an increase in the hemiacetal vibration peak at 887 cm^{-1} and a weakened –OH intensity support the conclusion that the aldehyde or hemiacetal groups were introduced into the celluloses by sodium periodate oxidation.

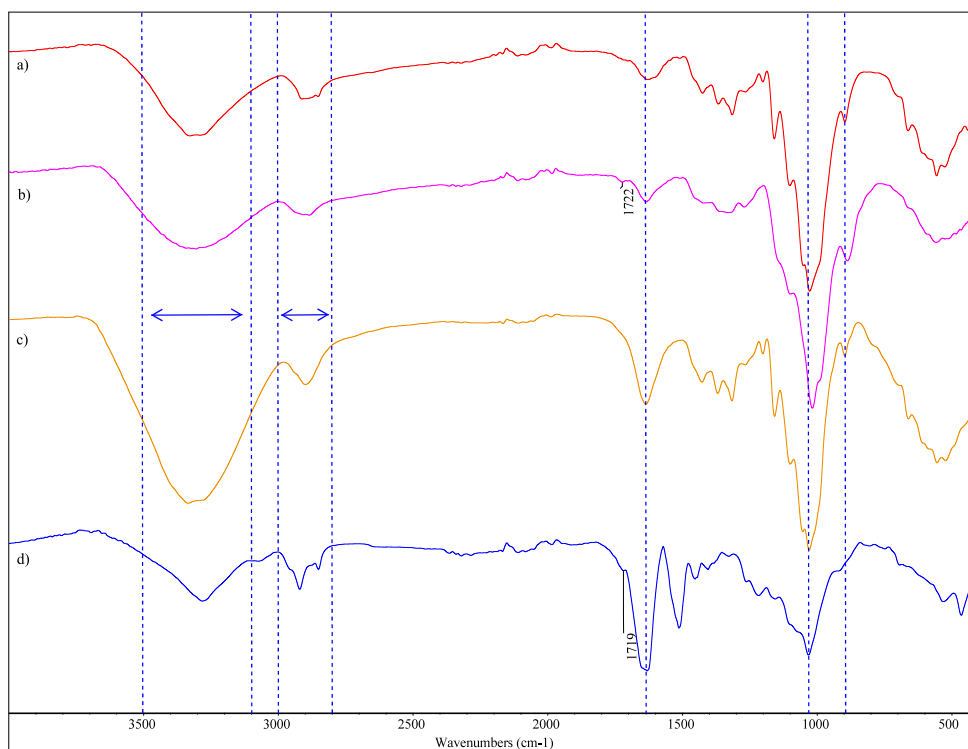


Figure 4.11: FTIR spectra of a) cellulose, b) DAC, c)CNC, and d) DANC.

Figure 4.12 shows the XRD patterns of cellulose and DAC. As previously determined, cellulose had distinct type I peaks that did not alter much following oxidation, showing that sodium periodate had a minimal effect on the nature of cellulose. The most noticeable DAC diffractions peaks were close to 16.6° and 21.9° , corresponding to the planes (110) and (200), respectively.¹³⁶ The less prominent one was for the plane (004) at a diffraction angle of 34.8° . However, for DAC, an appreciable reduction in the peaks of diffraction intensity was observed, indicating that the crystallinity may be disrupted by oxidation. The CI of DAC was 33.7%, notably smaller than the 84.4% obtained for nonoxidized cellulose. Thus, the calculated CI exhibited an evident effect of periodate oxidation on crystallinity reduction.

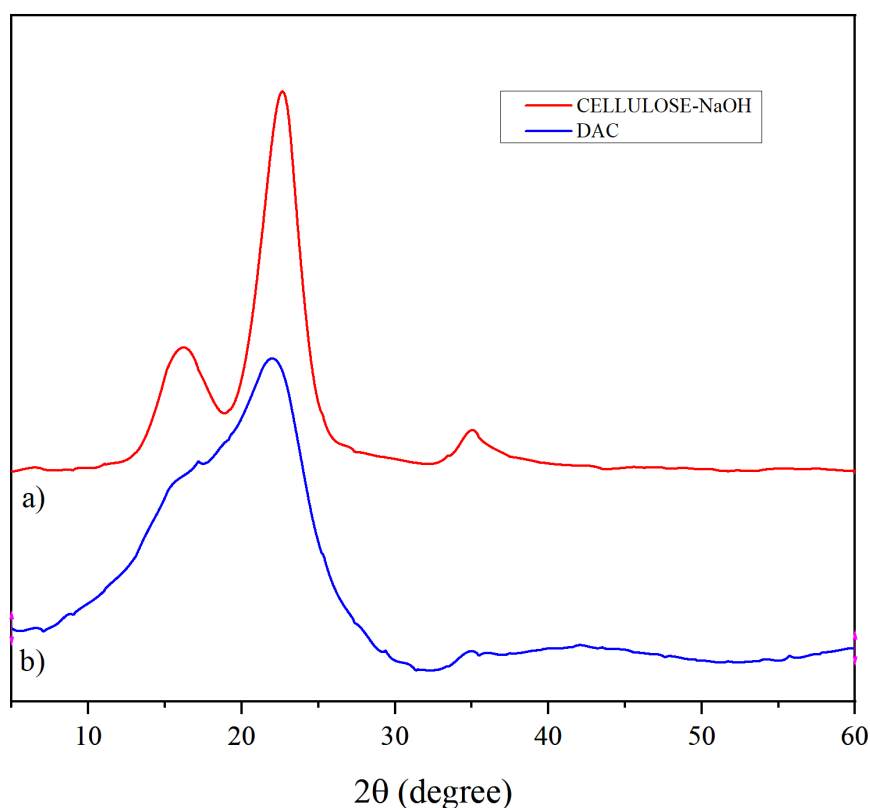


Figure 4.12: XDR diffraction pattern of (a) cellulose and (b) DAC.

4.5 Chitosan based biofilms

4.5.1 Film appearance and thickness

Chitosan is known for its film-forming ability. Chitosan filmed with various additives varies in their physicochemical properties. The solvent casting method of film formation, in which chitosan is first dissolved in an acidic media, blended with fillers and plasticizers, cast on plates, and air-dried to form films, is often used owing to its simplicity. Most

chitosan-based blends exhibited good film-forming ability in this study, making them easy to peel off from the Petri dishes. However, the film-forming ability of films was greatly influenced by the plasticizer content. There was a significant visual difference among CH films with variable glycerol amounts. The neat chitosan film was transparent, with many bubbles forming on the surface and slightly stiff. The addition of plasticizers improves the flexibility of films, but a more hygroscopic nature and yellowish tint were exhibited while increasing the quantity. CH/C2 with 2% glycerol was highly sticky and hygroscopic, making it hard to peel off. These films also exhibited a high degree of shrinking and deformation upon peeling Figure 4.13a. Therefore, a suitable glycerol percent was 0.5% Figure 4.13b. With the addition of CNC, the surface was smothered and less transparent than CH/C5. The material contracted and deformed after peeling. There was some large aggregation of CNC through the film due to the methodology used that did not reach a complete dispersion Figure 4.13c. All formed films formed with DANC were slightly brittle and showed yellow crystals through a very irregular surface Figure 4.13d. Those DANC agglomerations were visible and were the reason for opacity. After casting, CH/PCPH composite films in Figure 4.13e were not completely homogenous but presented good flexibility and transparency at lower PCPH percent. Due to the dark phenolic extract coloration, CH/PCPH/06 had a brownish tint.

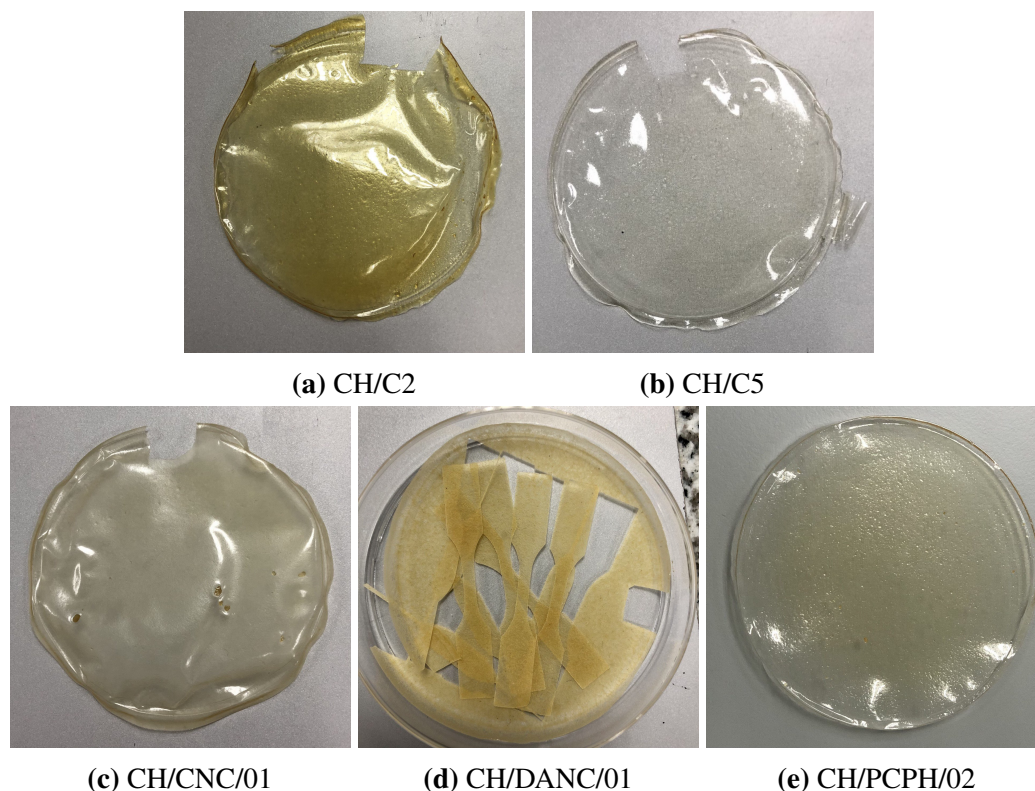


Figure 4.13: Photographs of chitosan-based films with different additives.

The thickness of chitosan control and formulated blend films varied from 0.049 to 0.229 mm, due to the interaction between chitosan and the different components. Table A.1 shows the increase in CH film thickness from 0.049 to 0.087 mm in response to the addition of 0.5% glycerol. It might be explained by plasticizers' action to modify the three-dimensional molecular organization of the polymer grid, reduce intermolecular attraction forces, and grow the free volume of the system.¹³⁷ With the addition of CNC or DANC, thickness also increases, possibly related to the strong interactions with the polymeric matrix through hydrogen bonding. Films incorporated with phenolic extracts tend to increase their thickness slightly at concentrations up to 5%. According to Perdones et al.,¹³⁸ this tendency is related to the higher solid content per surface unit. The results for concentrations lower than 1% are according to the ones reported by Souza et al.,¹³⁹ who demonstrated no significant difference in film thickness compared to the control. Qin et al.¹⁴⁰ revealed that the extract's phenolic compounds might have spreadability on the film surface without particularly changing the thickness.

4.5.2 FT-IR of films

FT-IR analysis attempted to characterize the effect of CNC, DANC, PCPH, and PT incorporation on the chitosan matrix and determine the infrared bands and shifts related to their interactions. The peaks in the chitosan film spectra Figure 4.14 are comparable to those described by other researchers.^{20,141-143} The broad absorption peak of the chitosan films at 3269 cm^{-1} is mainly assignable to the stretching of intra- and intermolecular O-H vibrations, overlapped with the N-H stretching. The absorption bands at 2925 and 2877 cm^{-1} correspond to the symmetric and asymmetric C-H stretching. The bands confirmed the presence of residual N-acetyl groups at around 1639 cm^{-1} (C=O stretching of amide I) and 1555 cm^{-1} (N-H bending of amide II). The absorption band at 1152 cm^{-1} belongs to the symmetric stretching of the C-O-C bridge. The bands at 1062 and 1024 cm^{-1} correspond to C-O stretching. Finally, the CH oop bending of the ring of monosaccharides corresponds to the signal at 896 cm^{-1} .

FTIR spectra peaks of pure CNC are described in section 4.2. Due to incorporating 3% and 5% CNC into the chitosan matrix, some differences can be observed in the FTIR spectra of chitosan films 4.14. With the addition of CNC, the absorption band at $3200\text{--}3400\text{ cm}^{-1}$ grew sharper and more intense, implying the formation of hydrogen bonds between chitosan and CNC, as confirmed by various authors.^{13,20,142} Enhancing the intensity at 1631 cm^{-1} peak also infers this bonding formation. A drastic increase in the intensity at 1062 and 1024 cm^{-1} confirms the incorporation of the CNC hydroxyl groups. Other changes in the spectra of the composite are minor. As the CH/CNC films contained glycerol, a new peak appeared at 923 cm^{-1} , suggesting the incorporation of the plasticizer into the

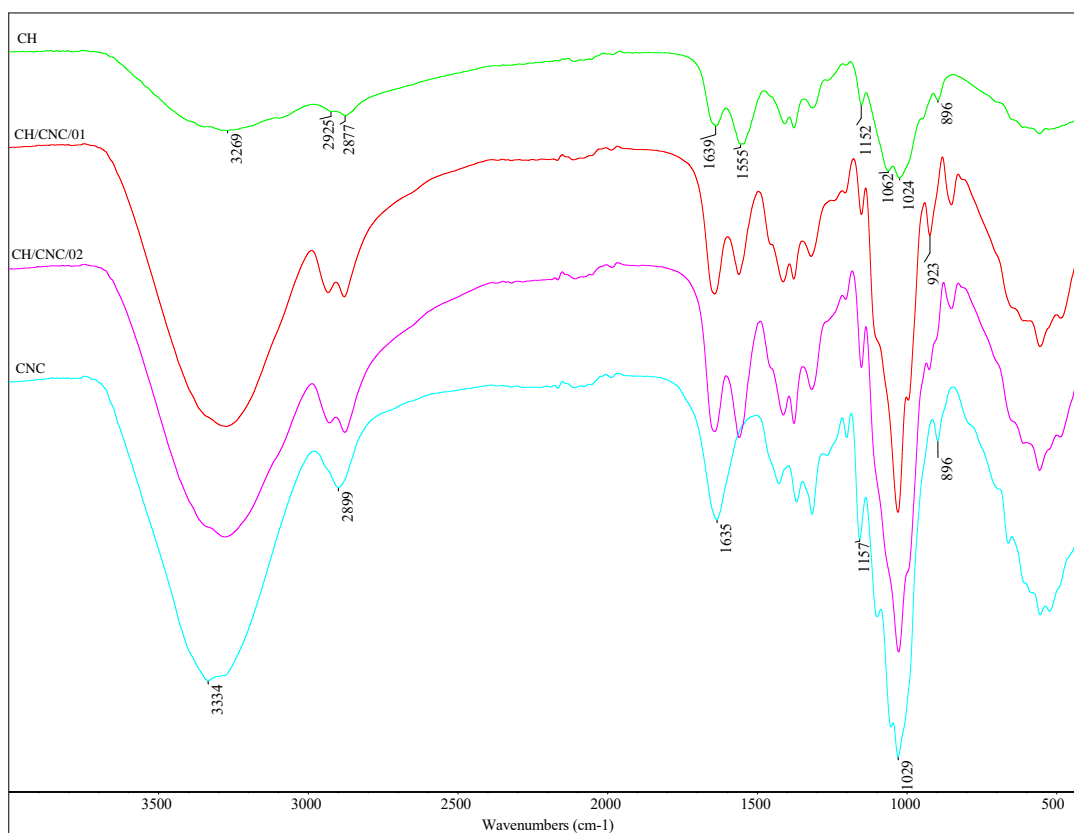
blend.¹⁴⁴

Figure 4.14: FTIR spectra of a) CH, b) CH/CNC/01, c) CH/CNC/02, and d) CNC.

The addition of DANC to the CH matrix changed the FTIR spectra 4.15. The periodate oxidation leads to the conversion of two hydroxyl groups in the C2 and C3 positions of glucose into aldehyde and carboxylic groups, as discussed in section 4.4. The N-acetyl groups of chitosan reacted with the aldehyde groups of DANC by a Schiff base formation. More aldehyde groups were linked to the amino group of chitosan when the DANC concentration was raised. After adding DANC into chitosan, the peak of DANC at 1719 cm^{-1} (aldehydic carbonyl groups) disappeared due to the Schiff base reaction. The -NH_2 stretching peak's intensity at 3346 cm^{-1} gradually decreased as the content of DANC increased. As the amount of DANC grows, the strength of the -NH_2 bending absorption band at 1555 cm^{-1} decreased dramatically. The Schiff base reaction produced a peak of -C=N stretching vibration at 1640 cm^{-1} that coincided with the C=O stretching in the amide I of chitosan. DANC and the chitosan matrix successfully blended, agreeing with the report by Gao et al.¹⁰⁰ that attributes the miscibility and compatibility of the two polymers to their similar structures. However, the DANC carboxylated part is expected to be incorporated into the matrix as a filler but can not be distinguished in the IR by

overlapping the Shift base peak.

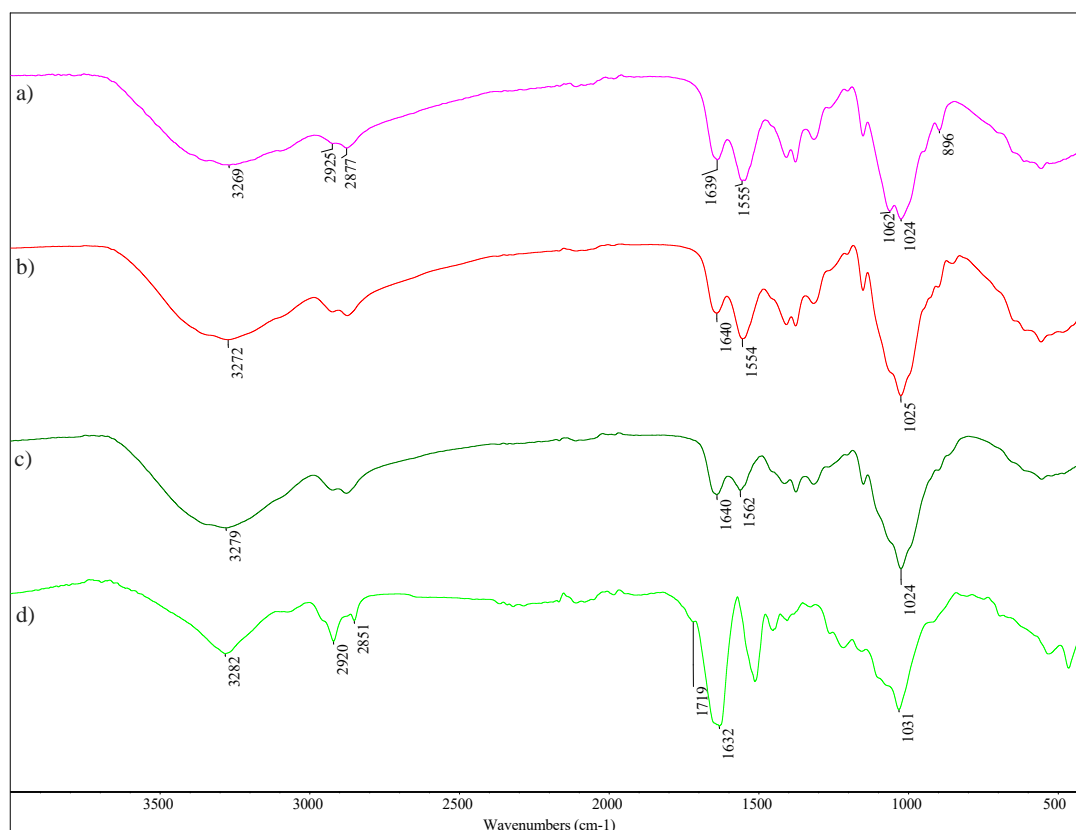


Figure 4.15: FTIR spectra of a) CH, b) CH/DANC/01, c) CH/DANC/02, and d) DANC.

The spectra of the CH/PCPh films at varied extract concentrations are shown in Figure 4.16, where no changes in FTIR spectra were observed. According to Pasanphan and Chirachanchai,¹⁴⁵ chitosan interacts with phenolic compounds via an amide bond, which is visible as an absorption peak at roughly 1620 cm^{-1} ; however, the chitosan band itself can mask it. According to Talón et al.,¹⁴⁶ the concentration of phenolic compounds in natural extracts is insufficient to produce a sensitive response in the spectra. The addition of PCPh, on the other hand, has been proven to affect the other properties discussed in the following sections.

4.5.3 Morphology of films

The distribution of aggregates, the existence of voids, the possible orientation of nanoparticles, and the degree of nanoparticle dispersion within the film may all be determined using SEM.¹⁰⁰ Figure 4.7 shows the SEM images of surfaces (a-c) and cross-sections (d-f) of chitosan-based films. Neat chitosan film has a smooth surface with some straps but no visible pores or cracks, indicating uniformity of the material 4.17a. The addition of DANC changed the film microstructure. The images show that DANC was dispersed

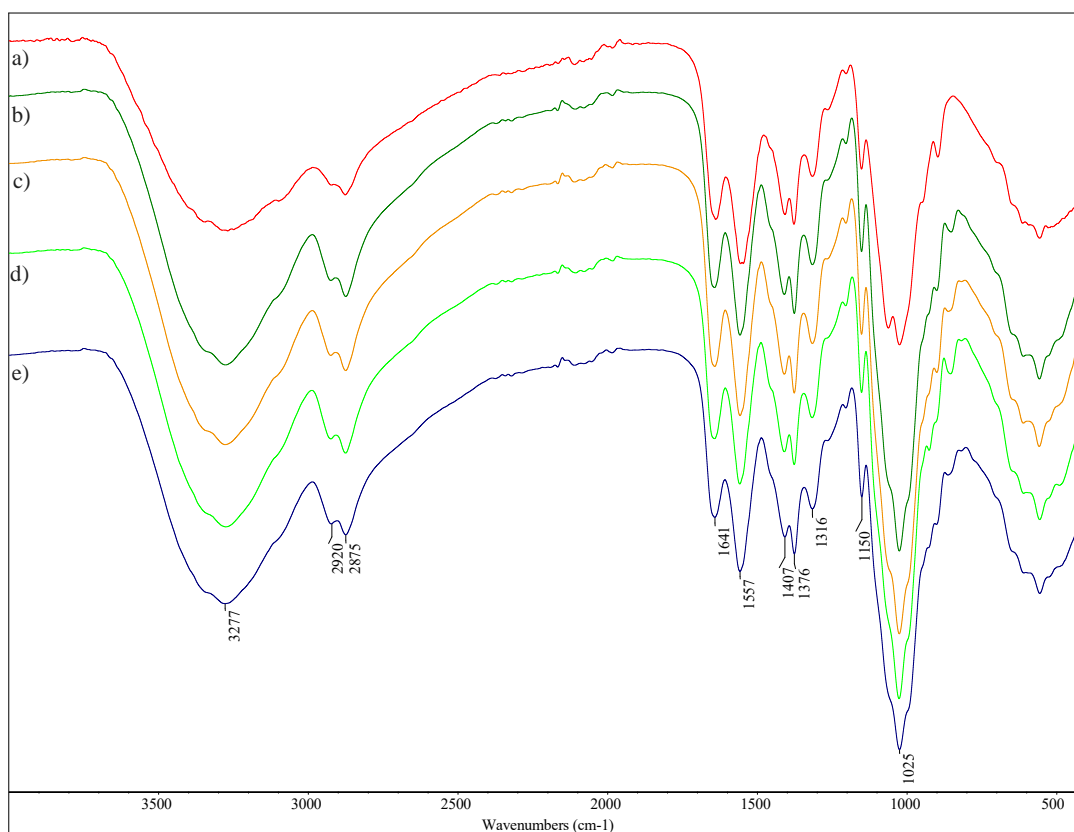


Figure 4.16: FTIR spectra of a) CH, b) CH/PCPH/01, c) CH/PCPH/02, d) CH/PCPH/05, and e) CH/PCPH/06.

within the chitosan matrix, and apparent DANC aggregation suggests a heterogeneous surface Figure 4.17c. It can be explained by the transversal sectioning of cellulose crystals.¹⁰⁰ In the CH/CNC film, CNC was evenly dispersed within the polymer matrix, and no apparent aggregation was evident, suggesting good compatibility between the polymer and the filler Figure Figure 4.17b. Cross-sectional images indicated that the pure chitosan film was smooth and compact in layers Figure 4.17d, whereas the incorporation of CNC and DANC resulted in some irregularities, such as multiple ripples and ridges on the edges of the film depicted in Figures 4.17e and 4.17f, respectively.

4.5.4 Mechanical properties of films

In order to evaluate the mechanical properties of chitosan-based films, tensile testing was carried out. The average values and standard deviation of the tensile strength (TS) and elongation at break ($\epsilon\%$) values are summarized in Table 4.1 and shown as bar charts in Figure 4.18. Depending on the type and percent variation of additive and glycerol, the tensile strength varied widely, ranging from 80 to 1.30 MPa. The pure chitosan film showed a larger value for TS of 80 MPa. This value can be attributed to the use of high molecular weight chitosan that tends to increase numbers of hydrogen bonding

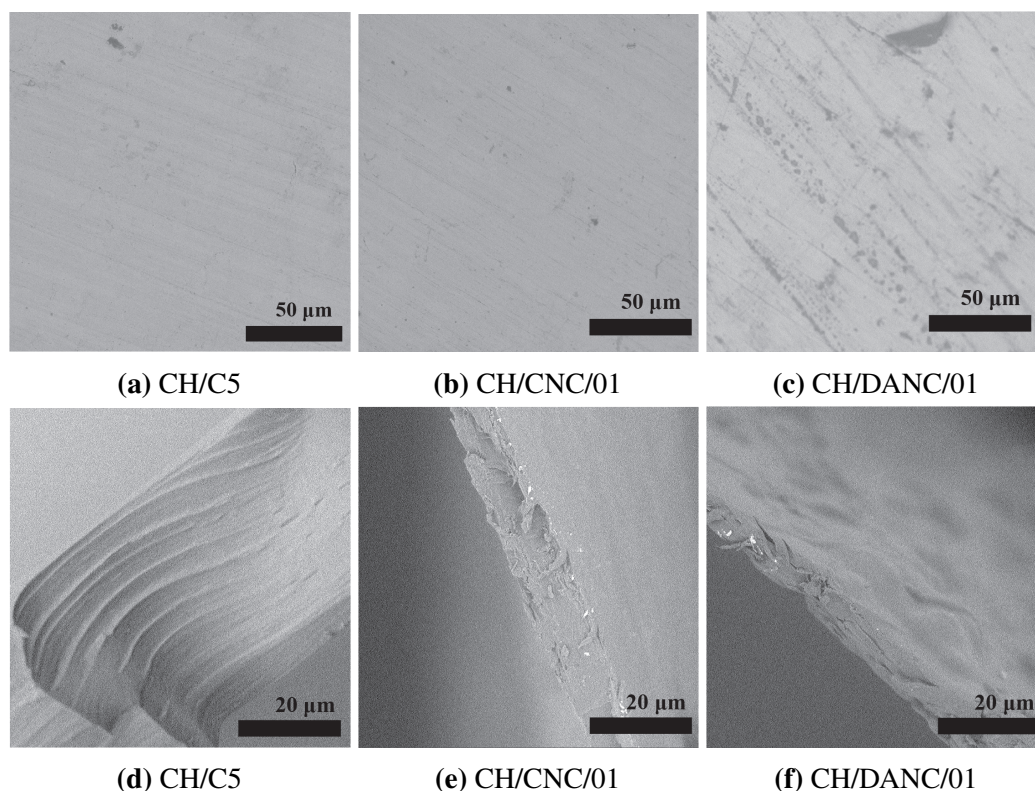


Figure 4.17: SEM images of chitosan-based films. (a–c) Surface morphology of films. (d–f) Cross sections of films.

attributed to the formation of higher tensile strength films.¹⁴⁷ Also, the preparation in acetic acid solution leads to a tighter structure than those prepared with other acid solutions. Nevertheless, the TS reduction was significantly high after adding glycerol as the plasticizer. Plasticizers are known to lower tensile strength, raise $\% \epsilon$, and make films more flexible while lowering toughness.¹⁴⁷ The addition of glycerol reduces intermolecular interactions between neighboring chitosan chains, resulting in increased free volume and decreased mechanical strength.¹⁴⁸ A higher glycerol concentration enables more sliding chains and boosts film elongation. At 2% glycerol, the films became oily and started to decompose quickly, enhanced by the humidity of the films, which was favored by the plasticizer content. Therefore, the mechanical test was not able to be conducted when the glycerol concentration increased. The most suitable glycerol concentration was 0.5%, used to evaluate the CPH-based additives blends.

The results show that the type and amount of additives employed impact the mechanical characteristics of chitosan films. The influences of additives on TS and $\% \epsilon$ are easily observed in Figure 4.18a and Figure 4.18b, respectively. Films made with CNC and PCPH at higher concentrations generally had significantly higher tensile strength values than the CH AND CH/DANC films. All films possessed a lower $\% \epsilon$ than the control one but Ch/DANC possessed a significantly lower $\% \epsilon$ than the other. These results suggest

Table 4.1: Tensile measurements of chitosan-based films.

Additive	Formulation	Tensile Strength (MPa)	Elongation to break (%)
	CH/C0	81 ± 24	6 ± 2
	CH/C5	16 ± 2	10 ± 1
	CH/C2	1.3 ± 0.3	0.24 ± 0.06
CNC	CH/CNC/01	11 ± 2	4.7 ± 0.4
	CH/CNC/02	33 ± 6	13 ± 3
DANC	CH/DANC/01	8.2 ± 0.45	1.23 ± 0.08
	CH/DANC/02	11 ± 6	0.94 ± 0.5
PHPC	CH/PCPH/01	38 ± 9	17 ± 3
	CH/PCPH/02	40 ± 9	17 ± 3
	CH/PCPH/05	7.0 ± 0.3	8.2 ± 0.5
	CH/PCPH/06	9 ± 4	8 ± 1

that CH/CNC and CH/PCPH films are suitable for forming flexible and tough films with chitosan and 2% glycerol. However, the CH/DANC films can be considered weak and brittle, accounting for lower tensile strength and $\% \epsilon$ values. These results for CH/DANC are not according to those presented by Gao et al.,¹⁰⁰ where they improved the tensile strength of the composite film with the highest TS value of 41.1 MPa at 25 wt.%, and $\% \epsilon$ of 2.79%. The results corroborate that due to the carboxylation of our CNC, the Schiff base is not formed. Crosslinking enhances the mechanical properties, but here, the additive possesses just a small aldehyde content to interact. The improvement in TS in CH/CNC film may be due to the electrostatic interactions and strong hydrogen bonding between the CNC and the CS matrix phase, which create an interactive network.^{16,99} Furthermore, the TS decreased from 35.40 ± 8.72 MPa to 11.26 ± 1.59 MPa when the loading amount of the CNC was increased from 3 to 5%. This drop may be attributed to the agglomeration of CNC in the CS matrix.¹⁶ The TS value for CH/CNC/02 is according to the 31 ± 2 MPa reported by Lavrič.⁹⁹ The different concentrations of PCPH influence the TS and $\% \epsilon$ results notoriously. Specifically, the addition of PCPH in 5% and 10% to the matrix decreased both mechanical properties compared to the control one. The decrease in mechanical properties might be due to the chitosan matrix's crystalline structure loss. Polyphenols in a film may disrupt the orderliness of crystal structure development, weakening intermolecular hydrogen bonds and obstructing polymer-polymer chain interactions.¹⁰¹ However, in pretty lower additions of 0.25% and 1.0%, a pretty significant increase in TS and $\% \epsilon$ is seen.

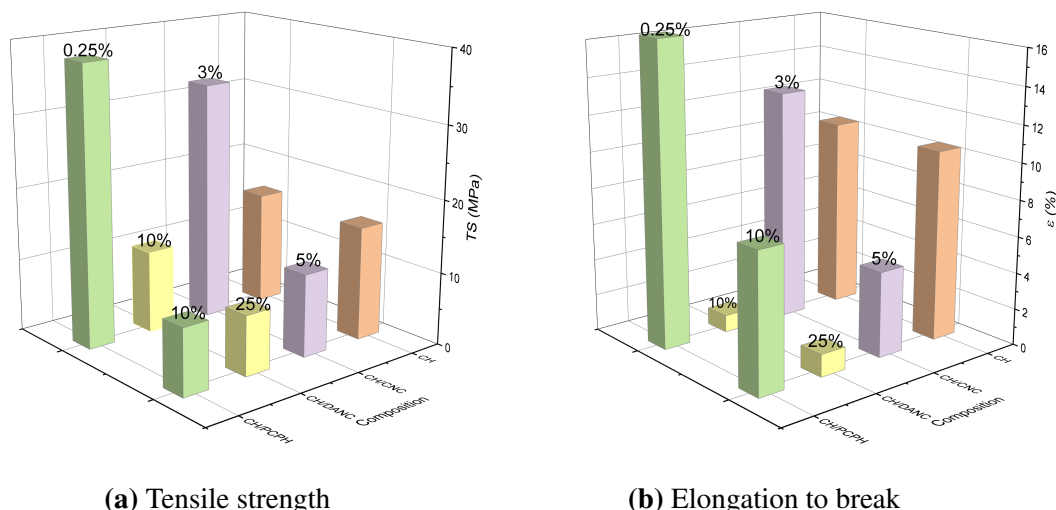


Figure 4.18: Mechanical properties of chitosan-based films made with different additives concentrations. The percent above the column represents the amount of additive per film.

These changes may be related to the hydrogen bonding between the chitosan's -NH and -OH groups and the functional groups in the PCPH.²⁹

According to Halim et al,¹⁴⁹ the tensile strength of traditional food packaging film requirements must be more than 3.5 MPa. Consequently, all chitosan-based films assessed may be considered appropriate for food packaging film based on their mechanical properties. But, due to its brittle behavior, we can discard DANC compositions.

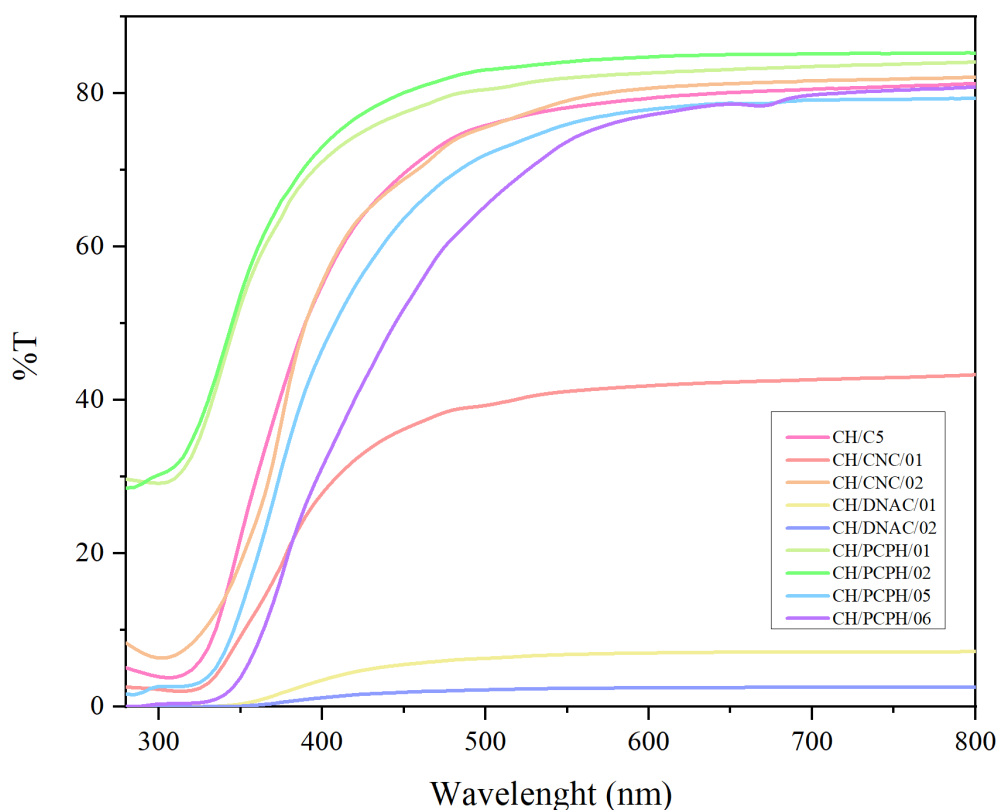
4.5.5 Optical properties of films

Transparency was evaluated throughout the samples' internal transmittance by scanning films in spectroscopy either on UV or visible light. As the final application is food packing, transparency is critical to improving product appearance and consumer acceptance.¹³⁹ Thus, incorporating different active compounds should not drastically decrease it. Figure 4.19a depicts the results of a spectroscopic scan of formed films measuring transmittance (%T) between 280 and 800 nm (UV–vis range). The films as a packaging material must protect food from exposure to light, particularly UV radiation since it confers extra protection against the oxidation process and possibly extends product shelf life. Pure chitosan film possesses an adequate barrier in the UV region (200–400 nm), where %T at 280 nm was 39.6%. However, by adding 0.5% of glycerol into the blend, the %T was reduced drastically to 5.08%. Mendoza et al.¹⁵⁰ demonstrated that this plasticizer exhibits a very high UV-blocking performance, abruptly decreasing %T after adding to the polymeric matrix.

Figure 4.19b contrasts the UV barrier block of all composites with 0.5% glycerol. The transmittance of CH/DANC films was lower than the chitosan control film and any other formulation, agreeing with the thickness results. Gao et al.¹⁰⁰ suggested that this

behavior could be related to the slight aggregation of DANC particles in the chitosan matrix that would increase the structural density of the film and thus scatter the light more intensely than the control film. The same tendency for CH/DANC is noticed in the visible region Figure 4.19c. In contrast, the CH films with the lowest content PCPH showed the highest light transmission than the other formulated films. However, the incorporation of natural antioxidants changed this barrier block on lower wavelengths at higher concentrations.¹³⁹ At 280 nm, the average amount of light blocked was much higher than the control film Figure 4.19b. In the case of CH/CNC films, due to the existence of the 3D structure of CNC, UV light absorption increases with increasing CNC, resulting in UV-resistant films, according to the demonstrated by Yadav et al.¹⁶

The greater the transmittance value at visible light, the better the transparency because more visible light can pass through the film. Higher opacity is equivalent to less transparency Table A.2.¹³⁹ The %T in the visible region (660 nm) for all films is presented in Figure 4.19c. As shown in Table A.2, adding low contents of CNC and PCPH does not significantly affect the film's transparency compared to control. Nevertheless, at higher concentrations, higher opacity is evident. The decrease in the light transmittance of the films may be mainly attributed to CNC agglomeration in the chitosan matrix.¹⁶ However,



(a) %T vs. Wavelength

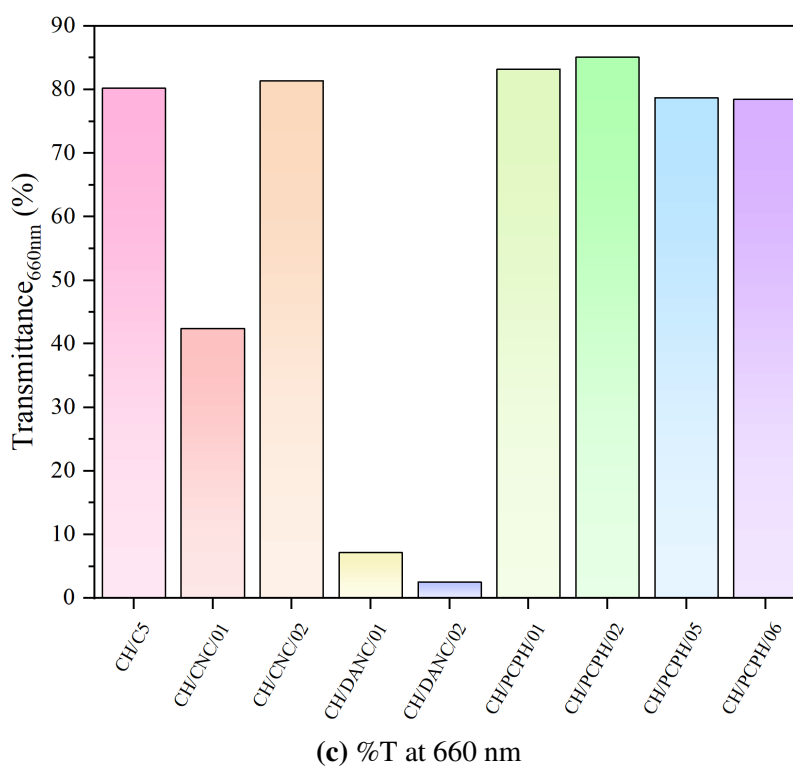
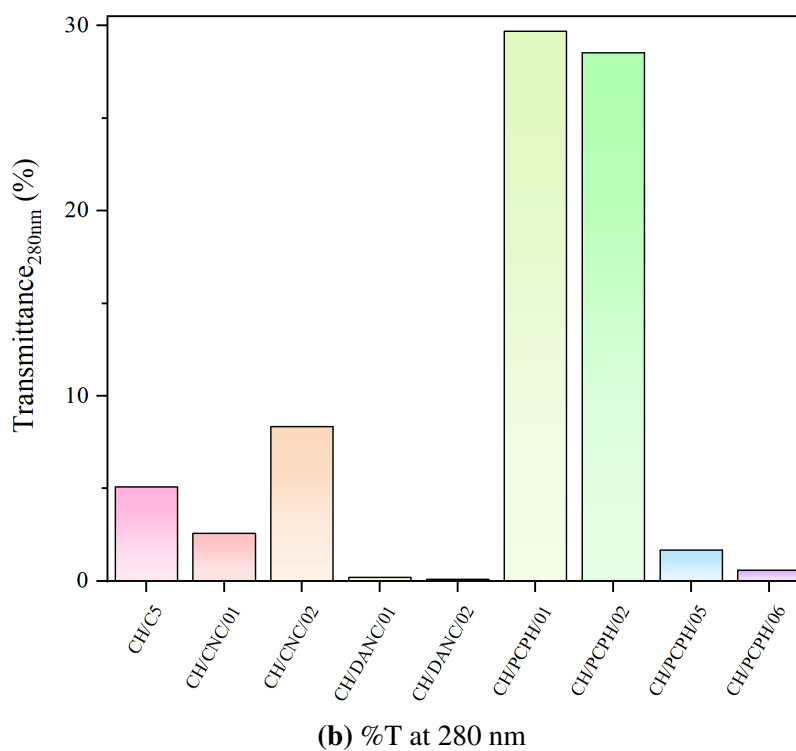


Figure 4.19: Optical transmittance (%T) of composite films.

in the PCPH case, some authors explain that the presence of phenolic compounds and their interaction with chitosan films generates an agglomeration in the matrix to produce a dark surface.³⁰ The same %T significant drop for CH/DANC is noticed in the visible region

Figure 4.19c. Compared to reported results,¹⁰⁰ this study's %T at 660 nm is lower, being attributed to the glycerol addition.

4.5.6 Swelling degree, solubility and moisture absorption

Because of the hydrophilic nature of chitosan, this polymer shows a high affinity toward the water. As a result, when chitosan films are hydrated, they absorb water and swell. The swelling behaviors of chitosan-based films are presented in Table 4.2. Chitosan pure film showed a higher degree of swelling, being 1656.90%. Chitosan films displaying such extreme swelling were reported beforehand.^{147,151} Reducing %SD is recommended for packaging purposes. The incorporation of glycerol led to more hydrogen bonds in the matrix film, which were responsible for the limited swelling behavior than the pure film. All the films prepared with glycerol showed lesser %SD than the values registered with neat chitosan, in agreement with the results presented by Debandi et al.¹⁴⁸ The hydrophilic character of the plasticizer allows for increased swelling as the amount of the plasticizer increases, which improves the dimensional stability of the films. There are hydrogen bonds between the glycerol molecules in high concentrations, involving the glycerol already bound to CH macromolecules, causing a clustering effect.¹⁴⁸ It was observed that the %SD of the CNC reinforced nanocomposite films (5% CNC) had been significantly reduced compared to the control chitosan film. CNC's low hydrophilicity and

Table 4.2: Swelling degree, solubility and moisture absorption of chitosan-based films.

Additive	Formulation	Swelling degree (%)	Solubility (%)	MA (%)
	CH/C0	1656.90	20.69	82.29
	CH/C3	223.08	64.90	36.23
	CH/C5	457.07	34.34	128.45
CNC	CH/CNC/01	106.08	46.49	70.25
	CH/CNC/02	373.51	31.35	125.71
DANC	CH/DANC/01	171.74	26.52	45.24
	CH/DANC/02	156.10	21.04	57.78
PCPH	CH/PCPH/01	1182.14	35.12	157.82
	CH/PCPH/02	742.03	34.30	170.18
	CH/PCPH/03	240.74	60.49	104.00
	CH/PCPH/04	130.58	59.63	105.99
	CH/PCPH/05	182.65	40.82	107.01
	CH/PCPH/06	242.53	35.63	101.69

strong filler-matrix interactions can explain the decrease in water uptake.¹⁴¹ CNC acted as an interpenetrated network inside the matrix, preventing the chitosan films from swelling when exposed to water. The CH/DANC composite films showed even lower %SD. It can be explained by chemical modifications that change surface functional groups and the crystallinity of cellulose and hence, its hydrophobicity. DANC has lower crystallinity but possesses surface groups like the carboxylic ones to form a sufficient amount of hydrogen bonds with the hydrophilic -OH groups of chitosan to form an effective shield against water, leading to improve hydrophobicity and decrease %SD.¹⁰⁰ According to Table 4.2, we can see the %SD of CH/PCPH film raised with the addition of CPH polyphenol extract due to its hydrophilic nature.¹⁵² However, %SD decreased while increasing the concentration of PCPH; it can be explained by the chitosan amide group bond with the polyphenols hydroxyl groups.¹³⁹

The water solubility percent of chitosan films is presented in Table 4.2. In the context of food packaging, %S is a critical metric since it allows for predicting the stability of films with high water resistance. Chitosan is insoluble in distilled water, but its solubility tends to rise while adding plasticizers and additives. Almost all the films maintained the original shape after being immersed in water; the ones containing more glycerol tended to roll themselves up. The CH films with a higher content of plasticizer increase its solubility significantly. By contrast, all the composites with chitosan 0.5% glycerol film can be distinguished a decrease in solubility for CNC and DANC containing films. This phenomenon can be explained by the CNC's 3D network structure, which prevents polymers from moving into water, resulting in a lower %S.¹⁶ Moreover, it could be attributed to hydrogen bonds between the CH matrix and DANC, which reduced its ability to absorb water. In the case of CH/PCPH, the solubility reduction was not observed, confirming that the interaction between chitosan and the extracts was not hydrophobic.

Moisture absorption from the air medium was tested, demonstrating hygroscopic behavior for all the films. The addition of glycerol again increases %MA. CH/C5 demonstrated moisture absorption of 128.45%, which decreased with CNC and DANC addition but tended to increase at low concentrations of PCPH. After a week, all films became more flexible on touch, and some of them presented some mold. %MA decreased to different scopes based on the concentration of fillers. The addition of 5% CNC reduced %MA to 70.25%, but the addition of lower concentrations do not show a substantial variation. In CH/DANC films also, a more considerable decrease of %MA is noticed for the composite with 25%. When PCPH increased from 0.25% to 10%, the %MA significantly decreased from 157.82% to 101.69 %, related to the electrostatic interactions and hydrogen bonding between PCPH and the matrix explained before.

4.5.7 Packing of blackberries

Fruits lose weight primarily due to their transpiration mechanism, which involves the transfer of water from cells to the atmosphere. Blackberries' high respiration rates help them lose weight by breaking down carbohydrates and organic acids. Rapid moisture loss to the surrounding air occurs due to the lack of a protecting rind or cuticle.¹⁵³ CH/DANC composite films have no potential to be applied as food wrapping materials due to their low flexibility and high stiffness. Figure 4.20 shows the storage of blackberries and their decays in the pure CH film and composites with CNC and PCPH. The blackberries present their characteristic red-purple color and smooth texture at day 0. After three days of storage, their physical appearance altered, becoming darker, especially those containing 5% PCPH. On day seven, weight loss is already notorious in all tested films and the ones without packaging. However, mold develops in the blackberries except for those stored in the low PCPH content films and the CNC reinforced ones. The hydrophobic nature of the CNC can explain it. For CH/PCPH films, the inhibition may be attributed to containing hydroxycinnamic acid. It has been reported that CPH extracts comprise this phenolic derivative which can inhibit Gram-positive and Gram-negative bacteria molds and yeasts.^{154,155} On day 17, all the samples lost weight completely and developed mold. A further studio of chitosan biocomposites with CNC and PCPH incorporation should be conducted to improve shelf storage.

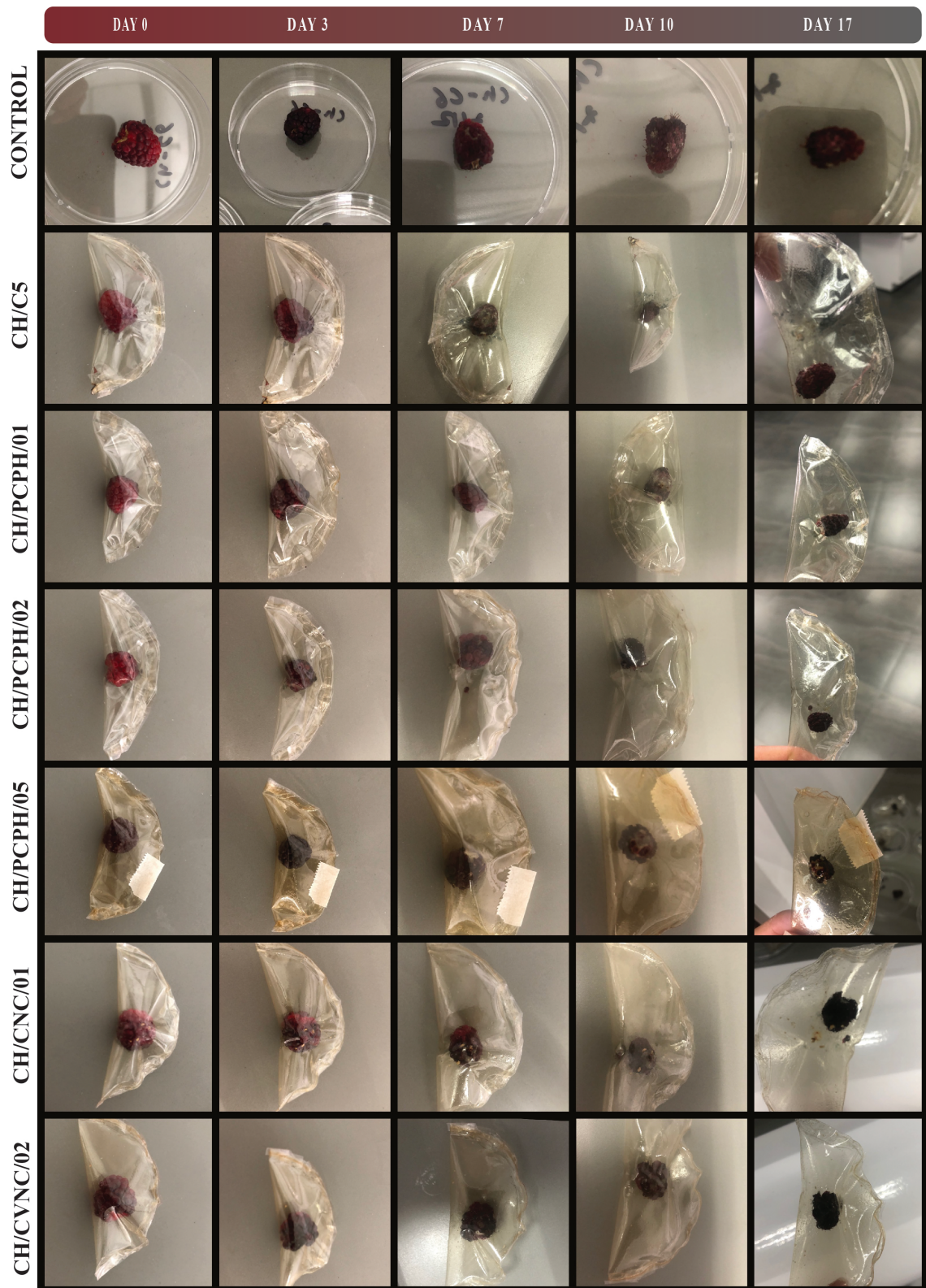


Figure 4.20: Effect of chitosan-based films packing on quality and shelf life of blackberries.

Conclusions and future work



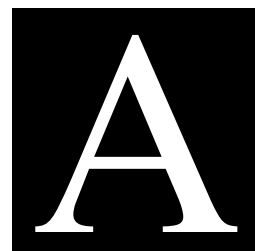
This work aimed to produce chitosan-based films reinforced with CPH extracted additives and evaluate their properties for possible application in food packing. In formulation, three different CPH-additives were used: CH/CNC, CH/DANC, and CH/PCPH. CNC, DANC, and PCPH addition were performed to enhance the materials barrier and mechanical properties and confirm their use as a promising barrier material in packaging applications. The concluding remarks are as follows:

- High crystalline cellulose (I) was successfully extracted from CPH by an alkali treatment followed by a bleaching step. The greener extraction methodology extracted pectin firstly and after the bleaching step holocellulose, showing lower crystallinity and confirming their identity by FTIR analysis.
- Enzymatic hydrolysis to obtain CNC was carried out correctly. The resulted CNC showed no change in chemical composition but a decrease in crystallinity. Microscopic studies exhibited porous and large irregularly shaped flakes.
- DAC and DANC were prepared through periodate oxidation under the same conditions. DAN aldehyde content was confirmed by FTIR analysis and a significant down in the CI. On the other hand, through its spectrum, DANC showed not only aldehyde groups but also carboxylate groups.
- Films of chitosan containing CPH additives were successfully prepared via the film casting method.
- FTIR analyses were conducted for all the compositions, confirming the incorporation of CNC in the chitosan matrix and the formation of the shift base between the chitosan amino group and the aldehyde of DANC.

- The thickness of CH/CNC and CH/DANC film increased as the content increased. However, the surface of CNC reinforced films was smooth forming and homogenized film, totally different from the heterogeneous surface of DANC film. Microscopic studies displayed evidence of DANC agglomeration on the microscale.
- The mechanical test implied a decreasing trend in tensile strength of pure CH films by adding glycerol as plasticizer and CPH additives. The suitable glycerol percent for chitosan formulations was 0.5% to enhance mechanical properties but not decompose due to the higher hygroscopicity. The CNC addition of 3% showed the most promising TS and $\% \epsilon$ features. Crosslinked and reinforced CH/DANC showed the lowest $\% \epsilon$, resulting from poor dispersion of the matrix material. Moreover, PCPH at lower quantities does not really affect the mechanical properties but up to 5% implies a decrease in TS.
- All film compositions proved to be good UV-blockers. Except for DANC formulations, the films presented lower opacities, giving them a suited appearance for food packing.
- Improved barrier properties of the materials were tested, resulting in the most favorable option, CH/CNC/02. There is a need to improve solubility in all cases. However, moisture absorption shows that some can be useful for specific dried food.
- PCPH formulated films reveal inhibition of mold growth, especially at 1% of phenolic concentration and 0.5% glycerol.

It is believed that modified chitosan films are proper alternatives for packaging purposes; hence, further developments in the nanocomposites' processing are promoted. To continue this work, improving the CNCs' distribution in the chitosan matrix is suggested to enhance the material's performance further. Furthermore, additives such as compatibilizers can be introduced into the matrix to improve the interactions between the matrix and nanocellulose-based fillers and improve the dispersion. It is also interesting to tailor the crosslinking process for DANC to induce an increase in tensile strength. Finally, further moisture studies such as WVTR (water vapor transmission rate), oxygen permeability, and thermogravimetric analysis properly the effect of water and gas diffusion and temperature on the material's performance.

Appendix



APPENDIX

Table A.1: Thickness of chitosan-based films.

Additive	Formulation	Thickness (mm)
	CH/C0	0.049 ± 0.012
	CH/C5	0.087 ± 0.019
CNC	CH/CNC/01	0.092 ± 0.018
	CH/CNC/02	0.111 ± 0.010
DANC	CH/DANC/01	0.212 ± 0.008
	CH/DANC/02	0.229 ± 0.012
PCPH	CH/PCPH/01	0.080 ± 0.008
	CH/PCPH/02	0.092 ± 0.005
	CH/PCPH/03	0.144 ± 0.007
	CH/PCPH/04	0.152 ± 0.005
	CH/PCPH/05	0.117 ± 0.012
	CH/PCPH/06	0.112 ± 0.017

Table A.2: Optical measures of chitosan-based films.

Additive	Formulation	%T₂₈₀	%T₆₆₀	Opacity (mm^{-1})
	CH/C0	39.6	87.14	1.15
	CH/C5	5.08	80.21	1.25
CNC	CH/CNC/01	2.59	42.43	2.36
	CH/CNC/02	8.34	81.34	1.23
DANC	CH/DANC/01	0.02	7.14	14.01
	CH/DANC/02	0.01	2.55	39.22
PHPC	CH/PCPH/01	29.69	83.21	1.20
	CH/PCPH/02	28.53	85.08	1.18
	CH/PCPH/05	1.68	78.69	1.27
	CH/PCPH/06	0.06	78.5	1.27

References

- (1) Peng, Y.; Wu, P.; Schartup, A. T.; Zhang, Y. *Proceedings of the National Academy of Sciences* **2021**, *118*, DOI: [10.1073/pnas.2111530118](https://doi.org/10.1073/pnas.2111530118).
- (2) Weber Macena, M.; Carvalho, R.; Cruz-Lopes, L. P.; Guiné, R. P. F. *Sustainability* **2021**, *13*, DOI: [10.3390/su13179953](https://doi.org/10.3390/su13179953).
- (3) Marsh, K.; Bugusu, B. *Journal of Food Science* **2007**, *72*, R39–R55.
- (4) Ncube, L. K.; Ude, A. U.; Ogunmuyiwa, E. N.; Zulkifli, R.; Beas, I. N. *Recycling* **2021**, *6*, DOI: [10.3390/recycling6010012](https://doi.org/10.3390/recycling6010012).
- (5) Ncube, L. K.; Ude, A. U.; Ogunmuyiwa, E. N.; Zulkifli, R.; Beas, I. N. *Materials* **2020**, *13*, DOI: [10.3390/ma13214994](https://doi.org/10.3390/ma13214994).
- (6) Vieira, M. G. A.; da Silva, M. A.; dos Santos, L. O.; Beppu, M. M. *European Polymer Journal* **2011**, *47*, 254–263.
- (7) Mellinas, C.; Ramos, M.; Jiménez, A.; Garrigós, M. C. *Materials* **2020**, *13*, DOI: [10.3390/ma13030673](https://doi.org/10.3390/ma13030673).
- (8) Bellich, B.; D'Agostino, I.; Semeraro, S.; Gamini, A.; Cesàro, A. *Marine Drugs* **2016**, *14*, 99.
- (9) Mohammadi Amirabad, L.; Jonoobi, M.; Mousavi, N. S.; Oksman, K.; Kaboorani, A.; Yousefi, H. *Carbohydrate Polymers* **2018**, *189*, 229–237.
- (10) Moeini, A.; Germann, N.; Malinconico, M.; Santagata, G. *Trends in Food Science and Technology* **2021**, *114*, cited By 9, 342–354.
- (11) Jiménez-Gómez, C.; Cecilia, J. *Molecules* **2020**, *25*, cited By 33, DOI: [10.3390/molecules25173981](https://doi.org/10.3390/molecules25173981).
- (12) Khan, R. A.; Salmieri, S.; Dussault, D.; Uribe-Calderon, J.; Kamal, M. R.; Safrany, A.; Lacroix, M. *Journal of Agricultural and Food Chemistry* **2010**, *58*, 7878–7885.

- (13) Mujtaba, M.; Salaberria, A. M.; Andres, M. A.; Kaya, M.; Gunyakti, A.; Labidi, J. *International Journal of Biological Macromolecules* **2017**, *104*, 944–952.
- (14) Ma, X.; Lv, M.; Anderson, D. P.; Chang, P. R. *Food Hydrocolloids* **2017**, *66*, 276–285.
- (15) Salari, M.; Sowti Khiabani, M.; Rezaei Mokarram, R.; Ghanbarzadeh, B.; Samadi Kafil, H. *Food Hydrocolloids* **2018**, *84*, 414–423.
- (16) Yadav, M.; Behera, K.; Chang, Y.-H.; Chiu, F.-C. *Polymers* **2020**, *12*, DOI: [10.3390/polym12010202](https://doi.org/10.3390/polym12010202).
- (17) Khan, A.; Khan, R. A.; Salmieri, S.; Le Tien, C.; Riedl, B.; Bouchard, J.; Chauve, G.; Tan, V.; Kamal, M. R.; Lacroix, M. *Carbohydrate Polymers* **2012**, *90*, 1601–1608.
- (18) Talebi, H.; Ghasemi, F.; Ashori, A. *Journal of Elastomers and Plastics* **2022**, *54*, cited By 0, 22–41.
- (19) Riccio, B.; Klosowski, A.; Prestes, E.; de Sousa, T.; de Assunção Morais, L.; Lemes, B.; Beltrame, F.; Campos, P.; Ferrari, P. *Journal of Applied Polymer Science* **2021**, *138*, cited By 3, DOI: [10.1002/app.50468](https://doi.org/10.1002/app.50468).
- (20) Kusmono; Wildan, M.; Lubis, F. *Polymers* **2021**, *13*, cited By 3, DOI: [10.3390/polym13071096](https://doi.org/10.3390/polym13071096).
- (21) Braga, D.; Bezerra, P.; Lima, A.; Pinheiro, H.; Gomes, L.; Fonseca, A.; Bufalino, L. *Polymers from Renewable Resources* **2021**, *12*, cited By 0, 46–59.
- (22) Gan, P.; Sam, S.; Abdullah, M.; Omar, M.; Tan, W. *Journal of Applied Polymer Science* **2020**, *137*, cited By 2, DOI: [10.1002/app.49578](https://doi.org/10.1002/app.49578).
- (23) Zhang, X.; Wei, Y.; Chen, M.; Xiao, N.; Zhang, J.; Liu, C. *Carbohydrate Polymers* **2020**, *246*, cited By 7, DOI: [10.1016/j.carbpol.2020.116489](https://doi.org/10.1016/j.carbpol.2020.116489).
- (24) Xu, Q.; Ji, Y.; Sun, Q.; Fu, Y.; Xu, Y.; Jin, L. *Nanomaterials* **2019**, *9*, cited By 43, DOI: [10.3390/nano9020253](https://doi.org/10.3390/nano9020253).
- (25) Tyagi, P.; Mathew, R.; Opperman, C.; Jameel, H.; Gonzalez, R.; Lucia, L.; Hubbe, M.; Pal, L. *Langmuir* **2019**, *35*, cited By 24, 104–112.
- (26) Adel, A.; El-Shafei, A.; Ibrahim, A.; Al-Shemy, M. *Journal of Renewable Materials* **2019**, *7*, cited By 10, 567–582.
- (27) Kõrge, K.; Bajić, M.; Likozar, B.; Novak, U. *International Journal of Food Science and Technology* **2020**, *55*, cited By 14, 3043–3052.
- (28) Zhang, X.; Liu, Y.; Yong, H.; Qin, Y.; Liu, J.; Liu, J. *Food Hydrocolloids* **2019**, *94*, cited By 113, 80–92.

- (29) Walid, Y.; Malgorzata, N.; Katarzyna, R.; Piotr, B.; Ewa, O.-L.; Izabela, B.; Wissem, A.-W.; Majdi, H.; Slim, J.; Karima, H.-N.; Dorota, W.-R.; Moufida, S.-T. *Journal of Food Processing and Preservation* **2022**, *46*, cited By 0, DOI: [10.1111/jfpp.16059](https://doi.org/10.1111/jfpp.16059).
- (30) Chan-Matú, D.; Toledo-López, V.; Vargas, M.; Rincón-Arriaga, S.; Rodríguez-Félix, A.; Madera-Santana, T. *Journal of Food Measurement and Characterization* **2021**, *15*, cited By 1, 4813–4824.
- (31) Kumar, N.; Pratibha; Trajkovska Petkoska, A.; Khojah, E.; Sami, R.; Al-Mushhin, A. *Materials* **2021**, *14*, cited By 2, DOI: [10.3390/ma14123305](https://doi.org/10.3390/ma14123305).
- (32) Severo, C.; Anjos, I.; Souza, V.; Canejo, J.; Bronze, M.; Fernando, A.; Coelho, I.; Bettencourt, A.; Ribeiro, I. *Food Packaging and Shelf Life* **2021**, *28*, cited By 6, DOI: [10.1016/j.fpsl.2021.100646](https://doi.org/10.1016/j.fpsl.2021.100646).
- (33) Rodrigues, M.; Bertolo, M.; Marangon, C.; Martins, V.; Plepis, A. *International Journal of Biological Macromolecules* **2020**, *160*, cited By 22, 769–779.
- (34) Nguyen, V.; Tran, T.; Tran, N. *Drying Technology* **2021**, cited By 1, DOI: [10.1080/07373937.2021.1913745](https://doi.org/10.1080/07373937.2021.1913745).
- (35) Rosenboom, J.-G.; Langer, R.; Traverso, G. *Nature Reviews Materials* **2022**, *7*, cited By 0, 117–137.
- (36) Alhawari, O.; Awan, U.; Bhutta, M.; Ali Ülkü, M. *Sustainability (Switzerland)* **2021**, *13*, cited By 39, 1–22.
- (37) Mellinas, C.; Ramos, M.; Jiménez, A.; Garrigós, M. *Materials* **2020**, *13*, cited By 57, DOI: [10.3390/ma13030673](https://doi.org/10.3390/ma13030673).
- (38) ICCO *Production of Cocoa Beans*; 2021.
- (39) ICCO *Cocoa Market Report - March 2021*; 2021, pp 1–5.
- (40) Oddoye, E.; Agyente-Badu, C.; Gyedu-Akoto, E., *Cocoa and its by-products: Identification and utilization*, cited By 29, 2013, pp 23–37.
- (41) Hennessey-Ramos, L.; Murillo-Arango, W.; Vasco-Correa, J.; Paz Astudillo, I. C. *Molecules* **2021**, *26*, DOI: [10.3390/molecules26051473](https://doi.org/10.3390/molecules26051473).
- (42) Santos, V.; Marques, N.; Maia, P.; de Lima, M.; Franco, L.; de Campos-Takaki, G. *International Journal of Molecular Sciences* **2020**, *21*, cited By 50, 1–17.
- (43) Pakizeh, M.; Moradi, A.; Ghassemi, T. *European Polymer Journal* **2021**, *159*, cited By 6, DOI: [10.1016/j.eurpolymj.2021.110709](https://doi.org/10.1016/j.eurpolymj.2021.110709).
- (44) Gropu, I. *Ecuador Shrimp Feed Market: Industry Trends, Share, Size, Growth, Opportunity and Forecast 2021-2026*; 2021.

- (45) Hong, L. G.; Yuhana, N. Y.; Zawawi, E. Z. E. *AIMS Materials Science* **2021**, *8*, 166–184.
- (46) Han, J., *A Review of Food Packaging Technologies and Innovations*, cited By 36, 2013, pp 3–12.
- (47) Halonen, N.; Pálvölgyi, P. S.; Bassani, A.; Fiorentini, C.; Nair, R.; Spigno, G.; Kordas, K. *Frontiers in Materials* **2020**, *7*, DOI: [10.3389/fmats.2020.00082](https://doi.org/10.3389/fmats.2020.00082).
- (48) Gómez-Gast, N.; López Cuellar, M. D. R.; Vergara-Porras, B.; Vieyra, H. *Polymers* **2022**, *14*, DOI: [10.3390/polym14061114](https://doi.org/10.3390/polym14061114).
- (49) Shaikh, S.; Yaqoob, M.; Aggarwal, P. *Current Research in Food Science* **2021**, *4*, 503–520.
- (50) Zhao, X.; Cornish, K.; Vodovotz, Y. *Environmental Science & Technology* **2020**, *54*, PMID: 32202110, 4712–4732.
- (51) Jeevahan, J.; Chandrasekaran, M. *Journal of Materials Science* **2019**, *54*, cited By 53, 12290–12318.
- (52) Parameswaranpillai, J.; Thomas, S.; Grohens, Y. In *Characterization of Polymer Blends*; John Wiley & Sons, Ltd: 2014; Chapter 1, pp 1–6.
- (53) Eletta, O.; Adeniyi, A.; Ighalo, J.; Onifade, D.; Ayandele, F. *Environmental Technology Reviews* **2020**, *9*, cited By 34, 20–36.
- (54) Okiyama, D.; Navarro, S.; Rodrigues, C. *Trends in Food Science and Technology* **2017**, *63*, cited By 94, 103–112.
- (55) Vásquez, Z.; de Carvalho Neto, D.; Pereira, G.; Vandenberghe, L.; de Oliveira, P.; Tiburcio, P.; Rogez, H.; Góes Neto, A.; Soccol, C. *Waste Management* **2019**, *90*, cited By 48, 72–83.
- (56) Meza-Sepúlveda, D.; Castro, A.; Zamora, A.; Arboleda, J.; Gallego, A.; Camargo-Rodríguez, A. *Agronomy* **2021**, *11*, cited By 1, DOI: [10.3390/agronomy11040693](https://doi.org/10.3390/agronomy11040693).
- (57) Jayeola, C.; Adebawale, B.; Yahaya, L.; Ogunwolu, S.; Olubamiwa, O., *Production of Bioactive Compounds From Waste*, cited By 3, 2018, pp 317–340.
- (58) Mendoza-Meneses, C.; Feregrino-Pérez, A.; Gutiérrez-Antonio, C. *Journal of Chemistry* **2021**, *2021*, cited By 0, DOI: [10.1155/2021/3388067](https://doi.org/10.1155/2021/3388067).
- (59) Vriesmann, L.; de Mello Castanho Amboni, R.; De Oliveira Petkowicz, C. *Industrial Crops and Products* **2011**, *34*, cited By 80, 1173–1181.
- (60) Figueroa, K. H. N.; García, N. V. M.; Vega, R. C. *Food Wastes and By-products* **2019**, 373–411.

- (61) Lu, F. et al. *Current Opinion in Green and Sustainable Chemistry* **2018**, *14*, cited By 41, 80–88.
- (62) Campos-Vega, R.; Nieto-Figueroa, K.; Oomah, B. *Trends in Food Science and Technology* **2018**, *81*, cited By 66, 172–184.
- (63) Daud, Z.; Awang, H.; Mohd Kassim, A.; Mohd Hatta, M.; Mohd Aripin, A. *Advanced Materials Research* **2014**, *911*, cited By 23, 331–335.
- (64) Nazir, N.; Novelina, .-.; Juita, E.; Amelia, C.; Fatli, R. *International Journal on Advanced Science, Engineering and Information Technology* **2016**, *6*, 403.
- (65) Chun, K.; Husseinsyah, S.; Osman, H. *Advances in Environmental Biology* **2014**, *8*, cited By 3, 2640–2644.
- (66) Chun, K.; Husseinsyah, S. *Journal of Thermoplastic Composite Materials* **2016**, *29*, cited By 22, 1332–1351.
- (67) Maulida; Maysarah, S.; Jose In cited By 1, 2020; Vol. 801.
- (68) Lubis, M.; Gana, A.; Maysarah, S.; Ginting, M.; Harahap, M. In cited By 14, 2018; Vol. 309.
- (69) Azmin, S.; Hayat, N.; Nor, M. *Journal of Bioresources and Bioproducts* **2020**, *5*, cited By 30, 248–255.
- (70) Wang, W.; Xue, C.; Mao, X. *International Journal of Biological Macromolecules* **2020**, *164*, cited By 52, 4532–4546.
- (71) Khayrova, A.; Lopatin, S.; Varlamov, V. *International Journal of Biological Macromolecules* **2021**, *167*, cited By 10, 1319–1328.
- (72) Azmana, M.; Mahmood, S.; Hilles, A.; Rahman, A.; Arifin, M.; Ahmed, S. *International Journal of Biological Macromolecules* **2021**, *185*, cited By 14, 832–848.
- (73) Alishahi, A.; Mirvaghefi, A.; Tehrani, M.; Farahmand, H.; Shojaosadati, S.; Dorkoosh, F.; Elsabee, M. *Journal of Polymers and the Environment* **2011**, *19*, cited By 30, 776–783.
- (74) El Knidri, H.; Belaabed, R.; Addaou, A.; Laajeb, A.; Lahsini, A. *International Journal of Biological Macromolecules* **2018**, *120*, 1181–1189.
- (75) Sanchez-Salvador, J.; Balea, A.; Monte, M.; Negro, C.; Blanco, A. *International Journal of Biological Macromolecules* **2021**, *178*, cited By 13, 325–343.
- (76) Aranaz, I.; Alcántara, A.; Civera, M.; Arias, C.; Elorza, B.; Caballero, A.; Acosta, N. *Polymers* **2021**, *13*, cited By 11, DOI: [10.3390/polym13193256](https://doi.org/10.3390/polym13193256).
- (77) Ma, T.; Hu, X.; Lu, S.; Liao, X.; Song, Y.; Hu, X. *Critical Reviews in Food Science and Nutrition* **2022**, *62*, cited By 12, 989–1002.

- (78) Kramar, A.; González-Benito, F. J. *Polymers* **2022**, *14*, DOI: [10.3390/polym14020286](https://doi.org/10.3390/polym14020286).
- (79) De Souza, T.; Kawaguti, H. *Food and Bioprocess Technology* **2021**, *14*, cited By 2, 1446–1477.
- (80) Khui, P.; Rahman, M.; Bakri, M. *Journal of Thermoplastic Composite Materials* **2021**, cited By 2, DOI: [10.1177/08927057211020800](https://doi.org/10.1177/08927057211020800).
- (81) Pasangulapati, V.; Ramachandriya, K. D.; Kumar, A.; Wilkins, M. R.; Jones, C. L.; Huhnke, R. L. *Bioresource Technology* **2012**, *114*, 663–669.
- (82) Radotić, K.; Mičić, M. In *Sample preparation techniques for soil, plant, and animal samples*; Springer: 2016, pp 365–376.
- (83) Ng, L. Y.; Wong, T. J.; Ng, C. Y.; Amelia, C. K. M. *Arabian Journal of Chemistry* **2021**, *14*, 103339.
- (84) Uusi-Tarkka, E.-K.; Skrifvars, M.; Haapala, A. *Applied Sciences (Switzerland)* **2021**, *11*, cited By 0, DOI: [10.3390/app112110069](https://doi.org/10.3390/app112110069).
- (85) Phanthong, P.; Reubroycharoen, P.; Hao, X.; Xu, G.; Abudula, A.; Guan, G. *Carbon Resources Conversion* **2018**, *1*, 32–43.
- (86) Wang, B.; Sain, M. *Composites Science and Technology* **2007**, *67*, 2521–2527.
- (87) Azeredo, H. M.; Rosa, M. F.; Mattoso, L. H. C. *Industrial Crops and Products* **2017**, *97*, 664–671.
- (88) Fortunati, E.; Luzi, F.; Puglia, D.; Dominici, F.; Santulli, C.; Kenny, J.; Torre, L. *European Polymer Journal* **2014**, *56*, 77–91.
- (89) Deng, Z.; Jung, J.; Zhao, Y. *LWT - Food Science and Technology* **2017**, *83*, 132–140.
- (90) Yu, Z.; Alsammarrarie, F. K.; Nayigiziki, F. X.; Wang, W.; Vardhanabhuti, B.; Mustapha, A.; Lin, M. *Food Research International* **2017**, *99*, 166–172.
- (91) Cao, L.; Sun, G.; Zhang, C.; Liu, W.; Li, J.; Wang, L. *Journal of Agricultural and Food Chemistry* **2019**, *67*, PMID: 30721049, 2066–2074.
- (92) Kargarzadeh, H.; Ahmad, I.; Abdullah, I.; Dufresne, A.; Zainudin, S.; Sheltami, R. *Cellulose* **2012**, *19*, 855–866.
- (93) Akinjokun, A. I.; Petrik, L. F.; Ogunfowokan, A. O.; Ajao, J.; Ojumu, T. V. *Heliyon* **2021**, *7*, DOI: [10.1016/j.heliyon.2021.e06680](https://doi.org/10.1016/j.heliyon.2021.e06680).
- (94) Rochina, D. DESIGN AND OPTIMIZATION OF A METHODOLOGY TO OBTAIN CELLULOSE AND CRYSTALLINE NANOCELLULOSE FROM OIL PALM EMPTY FRUIT BUNCH, Ph.D. Thesis, Yachay Tech, 2021.

- (95) Zhai, X.; Xiang, Y.; Tian, Y.; Wang, A.; Li, Z.; Wang, W.; Hou, H. *Journal of Vinyl and Additive Technology* **2021**, *27*, 781–794.
- (96) Sun, B.; Hou, Q.; Liu, Z.; Ni, Y. *Cellulose* **2015**, *22*, 1135–1146.
- (97) Wang, B.; Li, R.; Zeng, J.; He, M.; Li, J. *BioResources* **2021**, *16*, 1713–1725.
- (98) Cevallos, A. Cosmeceuticals products based on Cocoa Pod cellulose and Bioactive compounds with potential UV blocking activity, Ph.D. Thesis, Yachay Tech, 2021.
- (99) Lavrič, G.; Oberlintner, A.; Filipova, I.; Novak, U.; Likozar, B.; Vrabič-Brodnjak, U. *Polymers* **2021**, *13*, DOI: [10.3390/polym13152523](https://doi.org/10.3390/polym13152523).
- (100) Gao, C.; Wang, S.; Liu, B.; Yao, S.; Dai, Y.; Zhou, L.; Qin, C.; Fatehi, P. *Materials* **2021**, *14*, DOI: [10.3390/ma14195851](https://doi.org/10.3390/ma14195851).
- (101) Sun, L.; Sun, J.; Chen, L.; Niu, P.; Yang, X.; Guo, Y. *Carbohydrate Polymers* **2017**, *163*, 81–91.
- (102) Segal, L.; Creely, J.; A.E. Martin, J.; Conrad, C. *Textile Research Journal* **1959**, *29*, 786–794.
- (103) Panouillé, M.; Thibault, J.-F.; Bonnin, E. *Journal of Agricultural and Food Chemistry* **2006**, *54*, cited By 75, 8926–8935.
- (104) Dranca, F.; Oroian, M. *Molecules* **2019**, *24*, cited By 17, DOI: [10.3390/molecules24112158](https://doi.org/10.3390/molecules24112158).
- (105) Van Audenhove, J.; Bernaerts, T.; De Smet, V.; Delbaere, S.; Van Loey, A.; Hendrickx, M. *Foods* **2021**, *10*, cited By 2, DOI: [10.3390/foods10051064](https://doi.org/10.3390/foods10051064).
- (106) Belkheiri, A.; Forouhar, A.; Ursu, A.; Dubessay, P.; Pierre, G.; Delattre, C.; Djelveh, G.; Abdelkafi, S.; Hamdami, N.; Michaud, P. *Applied Sciences (Switzerland)* **2021**, *11*, cited By 4, DOI: [10.3390/app11146596](https://doi.org/10.3390/app11146596).
- (107) Acikgoz, C. *Asian Journal of Chemistry* **2011**, *23*, cited By 18, 149–152.
- (108) Wang, W.; Ma, X.; Jiang, P.; Hu, L.; Zhi, Z.; Chen, J.; Ding, T.; Ye, X.; Liu, D. *Food Hydrocolloids* **2016**, *61*, cited By 225, 730–739.
- (109) Zhang, L.; Ye, X.; Ding, T.; Sun, X.; Xu, Y.; Liu, D. *Ultrasonics Sonochemistry* **2013**, *20*, cited By 218, 222–231.
- (110) Pinto, E.; Aggrey, W. N.; Boakye, P.; Amenuvor, G.; Sokama-Neuyam, Y. A.; Fokuo, M. K.; Karimaie, H.; Sarkodie, K.; Adenutsi, C. D.; Erzuah, S.; Rockson, M. A. D. *Scientific African* **2022**, *15*, e01078.
- (111) Zhang, H.; Fu, S.; Chen, Y. *International Journal of Biological Macromolecules* **2020**, *147*, cited By 19, 607–615.
- (112) Kininge, M.; Gogate, P. *Ultrasonics Sonochemistry* **2022**, *82*, cited By 0, DOI: [10.1016/j.ultsonch.2021.105870](https://doi.org/10.1016/j.ultsonch.2021.105870).

- (113) Thomas, B.; Raj, M.; Athira, B.; Rubiyah, H.; Joy, J.; Moores, A.; Drisko, G.; Sanchez, C. *Chemical Reviews* **2018**, *118*, cited By 458, 11575–11625.
- (114) Yáñez-S, M.; Matsuhira, B.; Maldonado, S.; González, R.; Luengo, J.; Uyarte, O.; Serafine, D.; Moya, S.; Romero, J.; Torres, R.; Kogan, M. *Cellulose* **2018**, *25*, cited By 17, 2901–2914.
- (115) Bacci, L.; Di Lonardo, S.; Albanese, L.; Mastromei, G.; Perito, B. *Textile Research Journal* **2011**, *81*, cited By 48, 827–837.
- (116) Dassanayake, R.; Dissanayake, N.; Fierro, J.; Abidi, N.; Quitevis, E.; Bog-gavarappu, K.; Thalangamaarachchige, V. *Applied Spectroscopy Reviews* **2021**, cited By 0, DOI: [10.1080/05704928.2021.1951283](https://doi.org/10.1080/05704928.2021.1951283).
- (117) Trilokesh, C.; Uppuluri, K. *Scientific Reports* **2019**, *9*, cited By 75, DOI: [10.1038/s41598-019-53412-x](https://doi.org/10.1038/s41598-019-53412-x).
- (118) Rosli, N.; Ahmad, I.; Abdullah, I. *BioResources* **2013**, *8*, cited By 114, 1893–1908.
- (119) Maréchal, Y.; Chanzy, H. *Journal of Molecular Structure* **2000**, *523*, cited By 376, 183–196.
- (120) Abidi, N.; Cabrales, L.; Hequet, E. *Cellulose* **2010**, *17*, cited By 63, 309–320.
- (121) Cheng, S.; Huang, A.; Wang, S.; Zhang, Q. *BioResources* **2016**, *11*, cited By 35, 4006–4016.
- (122) Yang, X.; Berglund, L. *Advanced Materials* **2021**, *33*, cited By 22, DOI: [10.1002/adma.202001118](https://doi.org/10.1002/adma.202001118).
- (123) Hassan, M.; Berglund, L.; Abou Elseoud, W.; Hassan, E.; Oksman, K. *Cellulose* **2021**, *28*, cited By 0, 10905–10920.
- (124) Rovera, C.; Fiori, F.; Trabattoni, S.; Romano, D.; Farris, S. *Nanomaterials* **2020**, *10*, cited By 0, DOI: [10.3390/nano10040735](https://doi.org/10.3390/nano10040735).
- (125) Long, W.; Ouyang, H.; Hu, X.; Liu, M.; Zhang, X.; Feng, Y.; Wei, Y. *International Journal of Biological Macromolecules* **2021**, *186*, cited By 2, 591–615.
- (126) Zhang, Q.; Lu, Z.; Su, C.; Feng, Z.; Wang, H.; Yu, J.; Su, W. *Bioresource Technology* **2021**, *331*, cited By 4, DOI: [10.1016/j.biortech.2021.125015](https://doi.org/10.1016/j.biortech.2021.125015).
- (127) Cui, S.; Zhang, S.; Ge, S.; Xiong, L.; Sun, Q. *Industrial Crops and Products* **2016**, *83*, 346–352.
- (128) Boonsombuti, A.; Luengnaruemitchai, A.; Wongkasemjit, S. *Cellulose* **2013**, *20*, 1957–1966.
- (129) Banvillet, G.; Depres, G.; Belgacem, N.; Bras, J. *Carbohydrate Polymers* **2021**, *255*, cited By 7, DOI: [10.1016/j.carbpol.2020.117383](https://doi.org/10.1016/j.carbpol.2020.117383).

- (130) Rovera, C.; Ghaani, M.; Santo, N.; Trabattoni, S.; Olsson, R.; Romano, D.; Farris, S. *ACS Sustainable Chemistry and Engineering* **2018**, *6*, cited By 23, 7725–7734.
- (131) Abdallah, W.; Kamal, M. *Cellulose* **2018**, *25*, cited By 11, 5711–5730.
- (132) Mohamed, M. A.; W. Salleh, W.; Jaafar, J.; Ismail, A.; Abd Mutalib, M.; Mohamad, A. B.; M. Zain, M.; Awang, N. A.; Mohd Hir, Z. A. *Carbohydrate Polymers* **2017**, *157*, 1892–1902.
- (133) Sirvio, J.; Hyvakko, U.; Liimatainen, H.; Niinimäki, J.; Hormi, O. *Carbohydrate Polymers* **2011**, *83*, cited By 179, 1293–1297.
- (134) Liu, X.; Wang, L.; Song, X.; Song, H.; Zhao, J.; Wang, S. *Carbohydrate Polymers* **2012**, *90*, cited By 37, 218–223.
- (135) He, X.; Li, Y.; Zhang, L.; Du, R.; Dai, Y.; Tan, Z. *Cellulose* **2021**, *28*, cited By 1, 2833–2847.
- (136) Sirviö, J.; Liimatainen, H.; Niinimäki, J.; Hormi, O. *Carbohydrate Polymers* **2011**, *86*, cited By 50, 260–265.
- (137) Tarique, J.; Sapuan, S.; Khalina, A. *Scientific Reports* **2021**, *11*, cited By 16, DOI: [10.1038/s41598-021-93094-y](https://doi.org/10.1038/s41598-021-93094-y).
- (138) Perdonés, Á.; Vargas, M.; Atarés, L.; Chiralt, A. *Food Hydrocolloids* **2014**, *36*, 256–264.
- (139) Souza, V. G. L.; Fernando, A. L.; Pires, J. R. A.; Rodrigues, P. F.; Lopes, A. A.; Fernandes, F. M. B. *Industrial Crops and Products* **2017**, *107*, 565–572.
- (140) Qin, Y.-Y.; Zhang, Z.-H.; Li, L.; Yuan, M.-L.; Fan, J.; Zhao, T.-R. *Journal of Food Science and Technology* **2015**, *52*, cited By 72, 1471–1479.
- (141) Khan, A. DEVELOPMENT OF CELLULOSE NANOCRYSTAL REINFORCED ANTIMICROBIAL NANOCOMPOSITE FILMS FOR FOOD PACKAGING APPLICATION, Ph.D. Thesis, Université du Québec, 2014.
- (142) Costa, S.; Ferreira, D.; Teixeira, P.; Ballesteros, L.; Teixeira, J.; Figueiro, R. *International Journal of Biological Macromolecules* **2021**, *177*, cited By 15, 241–251.
- (143) Queiroz, M.; Melo, K.; Sabry, D.; Sasaki, G.; Rocha, H. *Marine Drugs* **2015**, *13*, cited By 302, 141–158.
- (144) Zhuang, J.; Li, M.; Pu, Y.; Ragauskas, A.; Yoo, C. *Applied Sciences (Switzerland)* **2020**, *10*, cited By 66, DOI: [10.3390/app10124345](https://doi.org/10.3390/app10124345).
- (145) Pasanphan, W.; Chirachanchai, S. *Carbohydrate Polymers* **2008**, *72*, cited By 162, 169–177.

- (146) Talón, E.; Trifkovic, K. T.; Nedovic, V. A.; Bugarski, B. M.; Vargas, M.; Chiralt, A.; González-Martínez, C. *Carbohydrate Polymers* **2017**, *157*, 1153–1161.
- (147) Nadarajah, K. Development and characterization of antimicrobial edible films from crawfish chitosan, Ph.D. Thesis, Louisiana State University, Agricultural, and Mechanical College, 2005.
- (148) Debandi, M. V.; Bernal, C. R.; Francois, N. **2016**, DOI: [10.4172/2157-7552.1000187](https://doi.org/10.4172/2157-7552.1000187).
- (149) Halim, A. L. A.; Kamari, A.; Phillip, E. *International Journal of Biological Macromolecules* **2018**, *120*, 1119–1126.
- (150) Mendoza, D.; Maliha, M.; Raghuwanshi, V.; Browne, C.; Mouterde, L.; Simon, G.; Allais, F.; Garnier, G. *Materials Today Bio* **2021**, *12*, 100126.
- (151) Nasef, M.; El-Hefian, E.; Saalah, S.; Yahaya, A. *E-Journal of Chemistry* **2011**, *8*, cited By 11, S409–S419.
- (152) Mayachiew, P.; Devahastin, S. *Food Chemistry* **2010**, *118*, 594–601.
- (153) Joshi, P.; Becerra-Mora, N.; Vargas-Lizarazo, A. Y.; Kohli, P.; Fisher, D. J.; Choudhary, R. *Future Foods* **2021**, *4*, 100091.
- (154) Martillanes, S.; Rocha-Pimienta, J.; Cabrera-Bañegil, M.; Martín-Vertedor, D.; Delgado-Adámez, J. In *Phenolic Compounds*, Soto-Hernandez, M., Palma-Tenango, M., del Rosario Garcia-Mateos, M., Eds.; IntechOpen: Rijeka, 2017; Chapter 3.
- (155) Belwal, T.; Cravotto, C.; Ramola, S.; Thakur, M.; Chemat, F.; Cravotto, G. *Foods* **2022**, *11*, DOI: [10.3390/foods11060798](https://doi.org/10.3390/foods11060798).